

GENEI RYODAN



Design, Build and FLY



Table of Contents

List of Figures	5
List of Tables.....	7
Nomenclature	8
1.0 Executive Summary	10
2.0 Management Summary	11
2.1 Team Organization	11
2.2 Project Milestones	12
3.0 Conceptual Design	12
3.1 Mission Requirements	13
3.1.1 Mission Constraints	13
3.1.2 System Requirements.....	13
3.1.3 Subsystem Requirements	14
3.2 Configuration selection	14
3.2.1 Wing Position.....	15
3.2.2 Wing Shape	16
3.2.3 Tail Geometry	16
3.2.4 Parachute Type selection.....	17
3.3 Final Conceptual Design Configuration	18
4.0 Preliminary design	19
4.1 Design Methodology	19
4.2 Design and Sizing	20
4.2.1 Assumptions.....	20
4.2.2 Geometries Estimation.....	20
4.2.3 Drag Estimation	22
4.2.4 Thrust Estimation.....	24
4.2.4.1 Static Thrust	24
4.2.4.2 Dynamic Thrust at cruise	24
4.2.4.3 Dynamic Thrust at maximum speed	24
4.3 Idesign (Graphical User Interface Program)	26
4.3.1 Program Function.....	26
4.3.2 Calculating Geometries.....	26
4.3.2.1 Program Inputs.....	26
4.3.2.2 Outputs	27
4.3.3 Estimating Thrust and Drag	27





4.3.3.1 Program Inputs.....	27
4.3.3.2 Program Outputs	28
4.3.4 Performance Calculations	28
4.3.4.2 Outputs	28
4.3.5 Program Simulation	29
4.4 Design and Sizing Trade Studies.....	32
4.4.1 Fuselage Design and Sizing	32
4.4.2 Airfoil Selection	33
4.4.2 Wing Design and Sizing.....	35
4.4.3 Tail Design and Sizing	35
4.4.3.1 Horizontal Tail	36
4.4.3.2 Vertical Tail.....	36
4.4.5 Control surface Design and sizing	36
4.4.5.1 Rudder.....	36
4.4.5.2 Elevator	36
4.4.5.3 Aileron.....	36
4.4.6 Parachute Sizing.....	37
4.4.7 Propulsion Sizing.....	38
4.5 Aircraft Stability Analysis	38
4.5.1 Static Stability.....	39
4.5.2 Dynamic Stability	41
5.0 Detailed Design.....	45
5.1 Dimensional parameters.....	45
5.2 Subsystem Design.....	46
5.2.1 Fuselage Skin.....	46
5.2.2 Internal Structures.....	47
5.2.3 Wing and Spars	49
5.2.4 Empennage and Tail Boom	50
5.2.5 Propulsion	51
5.2.6 Avionics and Wiring.....	51
5.3 Weight and Balance	51
5.4 Material Quantity	51
5.4.1 Internal Structure	51
5.4.2 Rods	52
5.4.3 Wing.....	53





5.4.4 Tail and Skin	53
5.4 Drawings	53
6.0 Manufacturing Plan.....	54
6.1 Manufacturing Processes Description.....	54
6.1.1 Hot Wire Cutting.....	54
6.1.2 Laser Cutting.....	54
6.1.3 3D Printing.....	56
6.2 Manufacturing Overview	56
6.2.1 Fuselage	56
6.2.2 Wings	57
6.2.3 Empennage.....	58
6.2.4 Electrical Components	58
6.2.5 Skin and Supply Box	59
7.0 Testing	60
7.1 Structural Test.....	60
7.2 Mechanisms and servos Test.....	62
7.3 Parachute Test	64
7.4 Flight Test	64
7.4.1 First Flight Test	65
8.0 Future Work	68
8.1 Aerodynamics	68
8.2 Propulsion	68
8.3 Structure	68
8.4 Manufacturing.....	68
9.0 References.....	69
10.0 MATLAB Code	70





List of Figures

Figure 1-Team Organization Chart	11
Figure 2- Gant Chart of The Team	12
Figure 3- Final Conceptual Design Configuration.....	18
Figure 4- Design Methodology Flow Chart	19
Figure 5-Geometry Tab Interface	29
Figure 6-Program Instructions.....	29
Figure 7-Geometery Results.....	30
Figure 8- Thrust and Drag Tab Interface.....	30
Figure 9- Thrust and Drag Results	31
Figure 10- Performance Tab Interface.....	31
Figure 11- Performance Results	32
Figure 12-Fuselage Sizing	33
Figure 13- Airfoil's Cl versus Alpha curves at different Reynold's number	34
Figure 14-Airfoil's Cd versus Alpha curves at different Reynold's number	34
Figure 15- Airfoils Cl/Cd versus Alpha curves at different Reynold's number.....	34
Figure 16- Forces affecting the Parachute.....	37
Figure 17- Propulsion Sizing Performance on eCalc.....	38
Figure 18- Aerodynamic Configuration on XFLR5	38
Figure 19-Cm and V Versus Alpha Curves of M1.....	39
Figure 20- Cn and Cl versus Beta curves of M1.....	40
Figure 21- Cn and Cl versus Beta curves of M2.....	40
Figure 22- V Versus Alpha Curve of M2.....	41
Figure 23-Longitudinal Pole Displacement of M1.....	41
Figure 24-Lateral Pole Displacement of M1.....	41
Figure 25- Flight Level Indicators	42
Figure 26- Longitudinal Velocity and Pitch angle Simulation of Phugoid Mode	42
Figure 27- Vertical Velocity and Pitch rate Simulation of short period mode.....	43
Figure 28- Side Velocity and Yaw rate of dutch mode simulation.....	43
Figure 29-Yaw rate Simulation of Spiral Mode	44
Figure 30- Roll rate Simulation of Roll Mode	44
Figure 31-Longitudinal Pole Displacement of M2.....	44
Figure 32-Lateral Pole Displacement of M2.....	44
Figure 33-Flight Levels Indicators.....	45
Figure 34- Skin Subsystem.....	46
Figure 35-Payload Dropping Mechanism.....	46
Figure 36- Fuselage Structural Components	47
Figure 37- Stopper and Battery Floor Structure.....	47
Figure 38-Motor Mount Structure	48
Figure 39- Supply Box Design	48
Figure 40- Wing and Spars Connection	49
Figure 41- Empennage and Boom Connection	50
Figure 42- Tail Connector Design	50
Figure 43- Hot Wire Cutting The Wing	54
Figure 44- Plywood Sheet Before Laser Cut Starting	55
Figure 45-Plywood Sheet After Laser Cutting	55
Figure 46- Skin After Laser Cutting	55





Figure 47- Tail Connector After Manufacturing	56
Figure 48- Fuselage Assembly	56
Figure 49- Wing and Airfoil	57
Figure 50- Spars and Boom Cutting.....	57
Figure 51- Ailerons Cutting.....	57
Figure 52-Tail Assembly.....	58
Figure 53- Tail's Servos Mounting	59
Figure 54- Aileron's Servo Mounting.....	59
Figure 55- Skin After Assembly	59
Figure 56- Flattened Skin Before Assembly.....	59
Figure 57-Manufactured Parachute	60
Figure 58- Manufacture Box.....	60
Figure 59- Succession of Motor Mount Test	61
Figure 60- Motor Mount Test Weight	61
Figure 61- Succession of Boom Deflection Test	62
Figure 62- Payload Box after being dropped.....	62
Figure 63- Payload Box before being dropped.....	62
Figure 64- Door Closing	63
Figure 65- Door Opening.....	63
Figure 66- Succession of Parachute Test	64
Figure 67- Aircraft weight before Propulsion installation	65
Figure 68- Avionics Testing	65
Figure 69- Hand Launched Aircraft	66
Figure 70- Takeoff Succession	66
Figure 71- High Maneuverability performance	67
Figure 72- Landing Succession	67





List of Tables

Table 1- Nomenclature Table	9
Table 2- Constraints of The Competition	13
Table 3-Mission Requirements and Constraints.....	14
Table 4- Sub-Systems Requirements	14
Table 5- Wing Position Decision Matrix	15
Table 6- Wing Shape Decision Matrix	16
Table 7- Tail Type Decision Matrix.....	17
Table 8- Parachute Shape Decision Matrix.....	18
Table 9- Airfoil Selection Decision Matrix	33
Table 10- Wing Parameters	35
Table 11- Horizontal Tail Parameters.....	36
Table 12- Vertical Tail Parameters	36
Table 13- Rudder parameters.....	36
Table 14- Elevator Parameters	36
Table 15- Aileron parameters.....	36
Table 16- Aircraft Stability Parameters of M1	42
Table 17- Stability parameters of M2.....	45
Table 18- Dimensional Parameters	46
Table 19- Balancing Components Displacements	51
Table 20- Structure Area, material and number of parts.....	52
Table 21- Structure Buy List	52
Table 22- Rods area, material and number of parts	52
Table 23- Rods Buy List.....	52
Table 24- Wing area, material and number of parts.....	53
Table 25- Wing Buy List	53
Table 26- Tail and Skin area, material and number of parts	53
Table 27- Tail Buy List	53





Nomenclature

AOA	Angle of attack
AR	Aspect ratio
b	Wingspan
b_a	Aileron Span
CAD	Computer Aided Design
C_a	Aileron Chord
C.G	Center of gravity
C_d	Coefficient of drag
C_{d_i}	Induced drag coefficient
C_f	Skin friction coefficient
C_{l_a}	Lift curve slope
$C_{l_{da}}$	Coefficient of lift due to aileron deflection
C_l	Coefficient of lift
C_{l_p}	Change of rolling moment coefficient with respect to roll rate
C_{m_a}	Change of pitching moment coefficient with respect to angle of attack
C_m	Pitching moment coefficient
C_{m_q}	Change of pitching moment coefficient with respect to pitch rate
C_{n_b}	Change of yawing moment coefficient with respect to sideslip angle
C_{n_r}	Change of yawing moment coefficient with respect to yaw rate
d_i	Spar inner diameter
d_o	Spar outer diameter
ESC	Electronic speed controller
KEAS	Knots equivalent air speed
KPP	Key performance parameters
L/D	Lift to drag ratio





MAC	Mean aerodynamic chord
MTOW	Maximum takeoff weight
N	Load factor
FOS	Factor of safety
HLD	High lift device
FF	Form factor
LIPO	Lithium Polymer
L_{spar}	Spar length
P	Concentrated load
P_r	Required power
R_e	Reynold number
ROC	Rate of Climb
RPV	Remotely Piloted Vehicles
S	Wing area
S_{ref}	Wing reference area
S_t	Tail area
S_{wet}	Wetted area
UAV	Unmanned aerial vehicle
V_a	Maneuvering speed
V_d	Diving speed
V_{max}	Maximum cruising speed
V_s	Stall speed
V_v	Vertical tail volumetric ratio
V_H	Horizontal tail volumetric ratio

Table 1- Nomenclature Table





1.0 Executive Summary

This report aims to detail how Team GENEI RYODAN whose name inspired from team in anime series taking the spider as an icon for the team. We have planned, designed, and manufactured a UAV that carries out the missions stated by the Unmanned Development Centre in its DBF Competition mission statement 2023. The sequence to be fulfilled in this year's competition is to take off with a payload, perform one complete lap around the course, drop the payload, perform one lap without the payload, and lastly land successfully and safely.

The development of this UAV technology can have different purposes: based on this year's competition theme, our UAV's mission is to drop a medical supply kit safely to the ground. This medical supply kit's size is 12cm x 12cm x 12 cm. The payload's weight includes the sum of both the supply kits and the parachute's weights. It is also required to make the UAV as lightweight as possible, to be safe for hand launching, and to be able to complete the mission in a time range of 3-5 minutes.

After researching more on medical UAVs used worldwide, we discovered a very important similarity between all different types: almost all medical UAV configurations are either single-boom, twin-boom, or simply a drone. This fact greatly helped us in narrowing down the configurations to choose from for our UAV and eliminating the conventional tail-connected configurations early on. In addition, drones are greatly slower than boomed aircraft, twin-boomed aircraft are generally heavier in weight than single-boomed aircraft and are mostly used for larger UAVs therefore, it was unchallenging to conclude that a single-boomed UAV would be most suitable for this year's mission statement.

Right after deciding on the configuration of our UAV in the preliminary design stage, it was required to design the most effective and high-performance propulsion sizing set and choose our wing and tail air foils after a few XFLR5 iterations. Our two biggest challenges during this stage were assuring that the stability margin for the UAV was relatively good and not close to the unstable region and having the lightest best-performing propulsion set.

During the detailed design stage, we faced more issues related to how to design the fuselage in a way to store the payload securely, and what we reached after a lot of trial and error with the internal structure was to design it with a truss pattern to hold the UAV body with as minimum weight as possible. The final design of our UAV ended up weighing about 1400g without payload and 2300g including the payload.





2.0 Management Summary

2.1 Team Organization

Our team was divided into different sub-teams according to which members felt most capable and knowledgeable in what fields. The team leader supervised all sub-teams and gave instructions regularly based on the DBF updates. Even though we were divided into sub-teams, all of us as a team filled each other's places and supported when necessary. Also, the team leader greatly helped all the sub-teams as well. The sub-teams divided were as follows: Aerodynamics Sub-team, Propulsion Sub-team, CAD Sub-team, Manufacturing Sub-team, Documentation Sub-team, and lastly all coding was done by Eslam Mahmoud. The chart below shows which team members were in each sub-team and are arranged from who worked the most to the least.

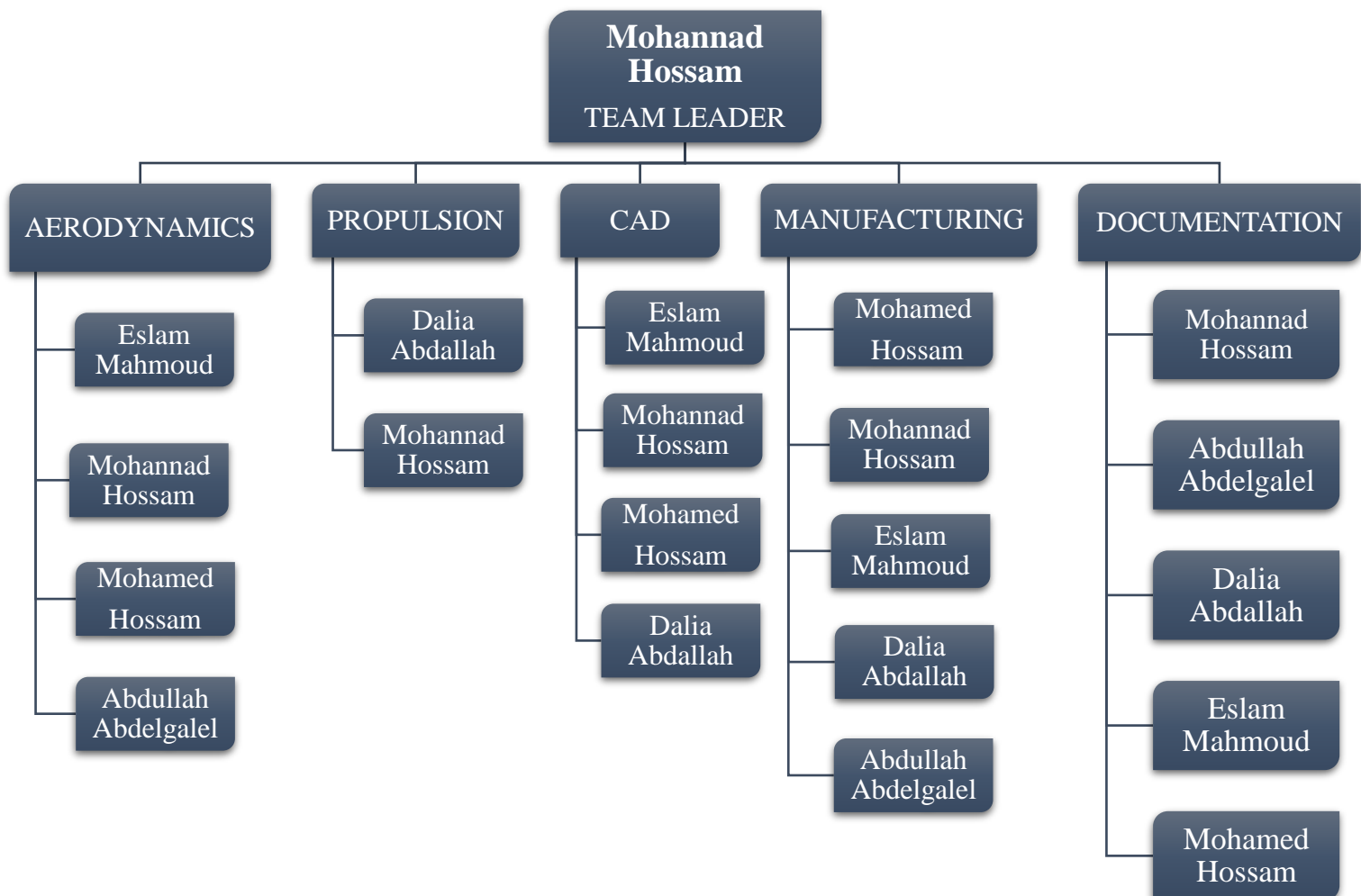


Figure 1-Team Organization Chart





2.2 Project Milestones

At the start of the 2023 summer a two-month schedule with all major events, milestones, and deliverables was outlined. Using past DBF team's performance as a guide, the schedule was constructed to allow three complete aircraft system-of-systems iterations and maximize the quality and score of this report. The schedule capitalized on parallel workflows wherever possible, providing each sub team with additional time to refine their deliverable with a soft transition between sub-teams. The team worked throughout summer holiday, with many meetings to obtain the best results. Figure 2 shows the major timelines and milestones.

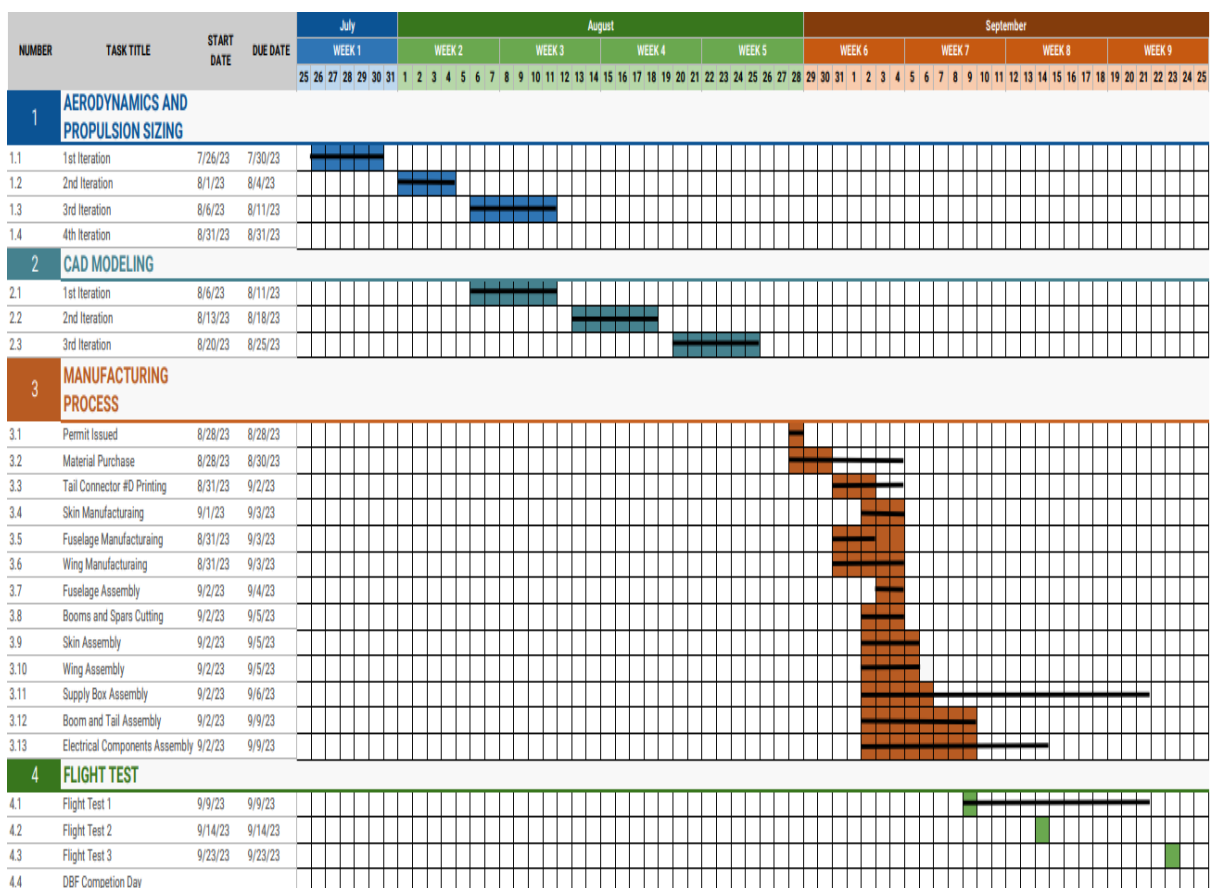


Figure 2- Gant Chart of The Team

3.0 Conceptual Design

The conceptual design includes a few aspects to consider at the beginning of designing our UAV before even choosing the configuration. The conceptual design stage simply analyzes everything we need to know about our UAV's mission and requirements. Those aspects include mission requirements and constraints and all the different systems and subsystems requirements as well. The following tables detail all the information we got during the conceptual design stage.





3.1 Mission Requirements

1. The UAV can be of any configuration, except quad-copter, rotary wing, or lighter-than-air. The UAV will be hand-launched (no landing gear will be used).
2. The UAV will have only one motor. The design must be suitable for hand-launching.
3. The design must be suitable for the parachute so it doesn't get stuck to the frame or the components.
4. The payload of the UAV should be composed of a box containing medical supplies.

3.1.1 Mission Constraints

MTOW (Maximum Take-Off Weight)	2.5 kg
Maximum Span	160 cm
Maximum airfoil thickness	4.5 cm
Box Dimensions (L x W x D)	12 x 12 x 12 cm

Table 2- Constraints of The Competition

3.1.2 System Requirements

System	Label	Mission Requirement
General Requirements	G1	The aircraft must be unmanned
	G2	The aircraft must be flown in the same configuration for all missions
	G3	The aircraft must be radio-controlled
	G4	The aircraft must be electric and propeller-driven
	G5	The batteries must be LiPo
	G6	Each team should design a propulsion system and a parachute
	G7	The aircraft must be capable of actuating all flight controls under the maximum weight.
	G8	The aircraft must not undergo any permanent deformation
	G9	The aircraft must fly 3 laps as fast as possible within the time of the propulsion system
	G10	The aircraft must carry a payload
	G11	The payload must have dimensions of 12x12x12 cm
	G12	The aircraft must have an external arming plug and avionics switch





	G13	The aircraft will be scored based on the weight applied and the maximum gross aircraft weight
	M1	Mission before dropping the box
	M2	Mission after dropping the box

Table 3-Mission Requirements and Constraints

3.1.3 Subsystem Requirements

Subsystem	Label	Mission Requirement
Aerodynamics Requirements	A1	The aircraft must be designed to conform to shipping container dimensions of $12+12+12=36\text{cm}$
	A2	The aircraft must generate sufficient lift in all flight regimes.
	A3	The aircraft configuration must minimize drag to allow for maximum possible speed.
Avionics and Propulsion	A.P1	The propulsion system must provide sufficient thrust to overcome drag in all flight configurations
	A.P2	The propulsion system must provide sufficient thrust to take off within 3 meters.
	A.P3	The propulsion system must at least have 10 minutes of endurance while maintaining optimum flight speed.
	A.P4	The avionics system should be easy to disable
	A.P5	The 5G sensor should experience no damage when the payload is dropped.
Structure	S1	All structural components must be able to withstand maximum load cases in all flight regimes.
	S2	The aircraft must be capable of withstanding a heavy point load without significant structural deformation
	S3	The aircraft must have a high strength-to-weight ratio

Table 4- Sub-Systems Requirements

3.2 Configuration selection

The following section details the design considerations made by the team throughout the conceptual design phase via weighted decision matrices. Each figure of merit was assigned a weight factor between 0 and 1 based on the impact each had on the final decision. A score between 0 and 3 was assigned to each configuration for each figure of merit, yielding a total score out of 3, with the optimal configuration having the highest score. To determine the weight and score of each component, research via trade studies and physical tests were performed. The configurations selected are outlined in green.





3.2.1 Wing Position

Three possible wing position configurations were considered: low, middle, and high wing. The figures of merit considered were stability, light weight, reduced drag, payload capacity, cruise performance, stall recovery and ergonomics which was defined as the aircraft's ability to store the electronics package and ease of access to it. Light weight and payload capacity were weighted more heavily due to the MTOW and the size of the box constraints and for sure high wing is not the lightest weight but it will be very effective to leave place for the payload (parachute and box). There is another very important points as stability and cruise performance, Lateral stability of any aircraft is highly affected by its wing placement. High wing placement proved to be the most reliable one, as the more the wings are moved down, the more instability would be encountered. Cruise performance also is an aircraft's performance in take-off, cruise and landing is all affected by the wing placement. Cruise performance is relatively poor for high wing aircrafts as they are more prone to an increase in profile drag as well as interference drag. However, for low-wing aircrafts the drag profile is much lower, resulting in a highly enhanced cruise performance. Nevertheless, the entire time-span of this mission is less than 5 minutes. Consequently, the high-wing's relatively poor cruise performance is not considered an obstacle and thereby, as seen in the table below, the cruise performance criteria as only awarded a scale factor of 0.1.

Figure of merit	Factor	Low wing	Mid wing	High wing
Payload Capacity	0.2	3	1	3
Ergonomics	0.15	3	1	3
Light weight	0.15	3	1	2
Stability	0.15	0	2	3
Reduced drag	0.15	2	3	2
Cruise performance	0.1	3	1	2
Stall recovery	0.1	3	2	2
Total Score	1	2.4	1.55	2.5

Table 5- Wing Position Decision Matrix





3.2.2 Wing Shape

Four wing shapes were considered: straight, tapered and swept. The figures of merit were manufacturability, lift, stability, drag and weight. The manufacturability was prioritized. High lift was prioritized next to carry the payload. Stability and drag are equally weighted, the most stable configuration by maximizing wing area and aspect ratio. Minimizing drag was also critical to improving performance. Therefore, while the Swept would have better performance as it gives more stability and less drag, its difficulty to manufacture made it disadvantageous, leading to a straight wing being our choice.

Figure of merit	Factor	Straight Shape	Tapered Shape	Swept Shape
Manufacturability	0.35	3	2	1
Lift	0.25	3	2	1
Stability	0.2	1	1	3
Drag	0.15	1	2	3
Weight	0.1	1	2	3
Total Score	1	1.95	1.9	1.95

Table 6- Wing Shape Decision Matrix

3.2.3 Tail Geometry

Three tail configurations were considered: conventional, cruciform and t-tail. The figures of merit considered were drag, weight, stability, structural easiness, ease of manufacturing, control complexity and stall recovery. Stability was considered the most important aspect, being the primary role of the tail. Control complexity considered controlling the control surfaces by servo motor. Manufacturability took into account too. Low drag and weight were treated as lower priorities due to the tail's relatively small size compared to the rest of the aircraft. Structural complexity is the complexity of the structural elements required to construct the part to be rigid. Considering this, the conventional configuration achieved first place. Team decided on the conventional configuration for design simplicity and assembly time.





Figure of merit	Factor	Conventional	T-tail	Cruciform
Structural easiness	0.25	3	1	2
Weight	0.25	3	1	2
Stability	0.15	1	3	2
Drag	0.15	3	1	2
Manufacturability	0.1	3	1	2
Stall recovery	0.1	3	1	2
Total Score	1	2.55	1.3	2

Table 7- Tail Type Decision Matrix

3.2.4 Parachute Type selection

A parachute can control the model's descent speed more accurately and bring the model down more slowly than any other recovery method. The best parachutes are made from strong, thin, soft, flexible material. For small models, thin plastic sheets work very well because they can be folded up tightly to fit into small diameter body tubes. Some sources for parachute canopies include: Mylar, plastic drop cloths, dry-cleaning bags, trash bags, and gift-wrapping plastic. For Weight with a descent mass greater than 300 grams a cloth material like cotton, silk, polyester, or nylon is used. These materials can withstand the larger opening forces that bigger models can create. After searching there were four main types of parachutes which are cross, square, flat circular and hemisphere, each one has different characteristics, drag coefficient is the most important characteristic as this characteristic will keep us committed with the constraint of not triggering the shock sensor, stability comes next as it's very important that the box lands safely and we took manufacturability and weight in less consideration. The following table shows the characteristic and the chosen type of parachute.





Figure of merit	Factor	Cross	Square	Hemisphere	Flat Circular
Drag Coefficient	0.4	1	2	3	3
Stability	0.3	3	2	2	1
Manufacturability	0.15	3	2	2	1
Weight	0.15	3	1	1	2
Total Score	1	2.2	1.85	2.25	1.95

Table 8- Parachute Shape Decision Matrix

3.3 Final Conceptual Design Configuration

The final GR-UAV configuration is a high wing, conventional boom tail, straight wing aircraft. It features no twist or dihedral beside high aspect ratio. With winglets which decrease downwash effect and increase spiral stability. The parachute comes with a spill hole in a hemisphere geometry with nylon material.

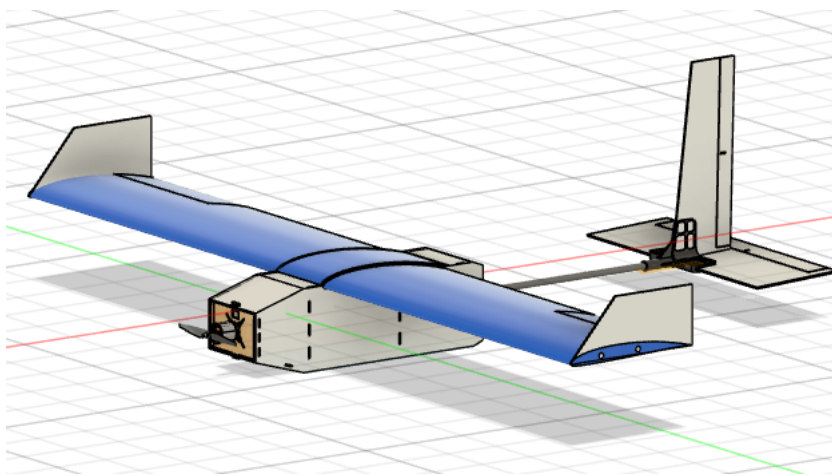


Figure 3- Final Conceptual Design Configuration





4.0 Preliminary design

The outcome of the preliminary design phase was a set of specifications and drawings that were used as a basis for the detail design phase, which involved the finalization of the design and the preparation of manufacturing drawings and other detailed engineering documentation.

4.1 Design Methodology

The design and analysis methodology used was built on the experience from prior competition cycles and advice from mentors. Subsequently, different configurations were modelled using Fusion 360 and the propulsion estimation tool eCalc. These design concepts were weighed against each other and narrowed down. All calculations for sizing are done using a tool that we have built to increase the efficiency and decrease the consumed time. Our preliminary analysis provided first estimates on expected aircraft performance, allowing for an aerodynamic prototype to be built to validate the design. Further detailed analysis was performed in XFLR5. All the trials are conducted taking into the consideration the constraints. The following chart shows the process of the design.

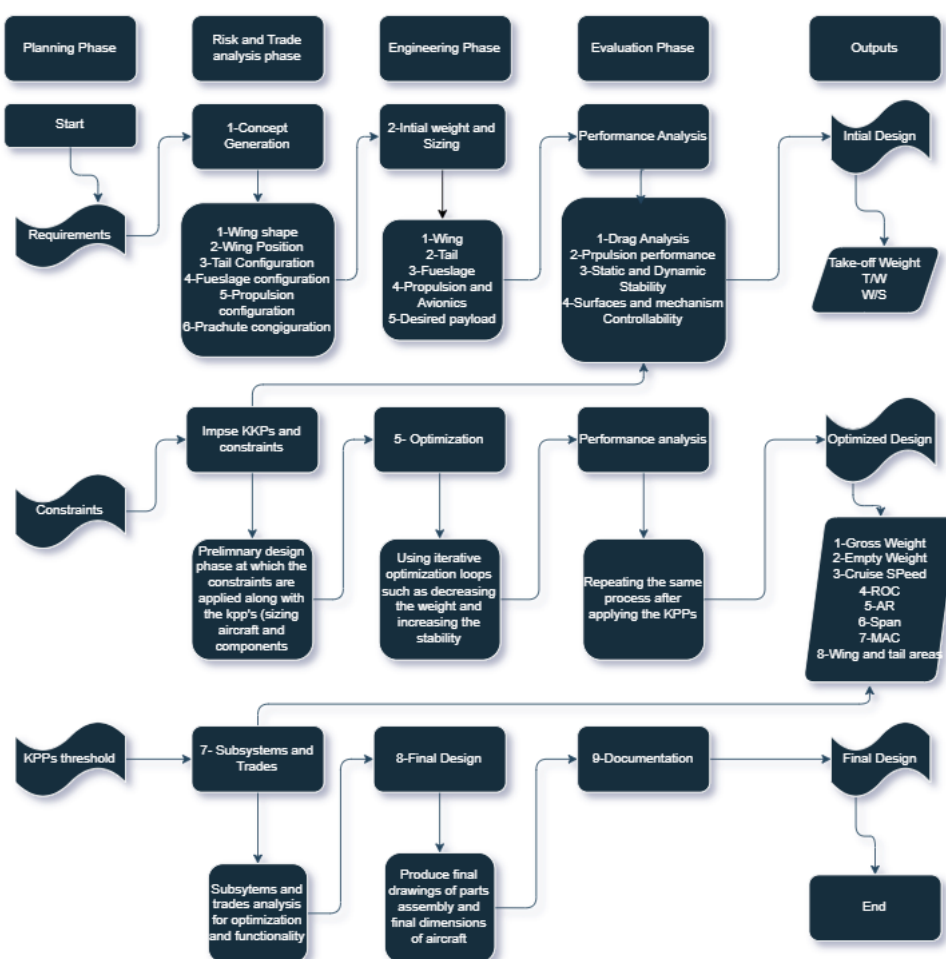


Figure 4- Design Methodology Flow Chart

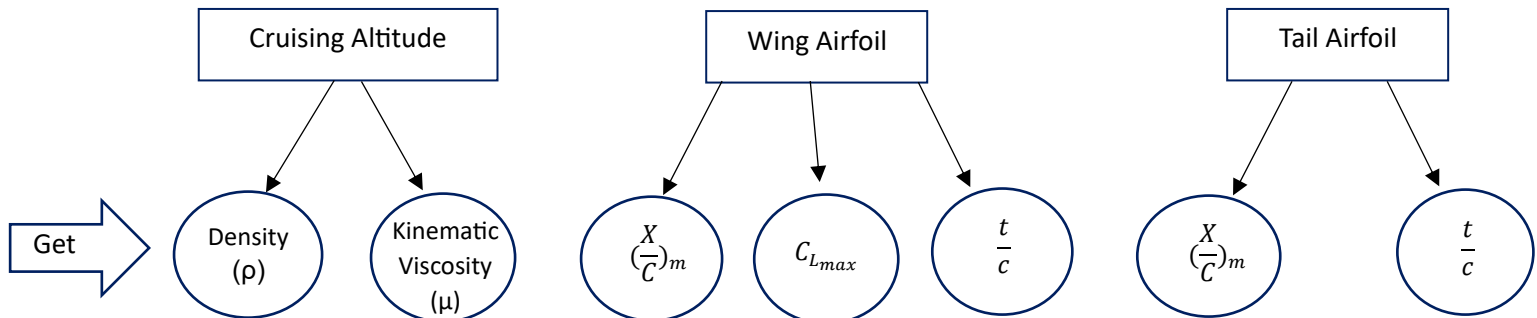




4.2 Design and Sizing

4.2.1 Assumptions

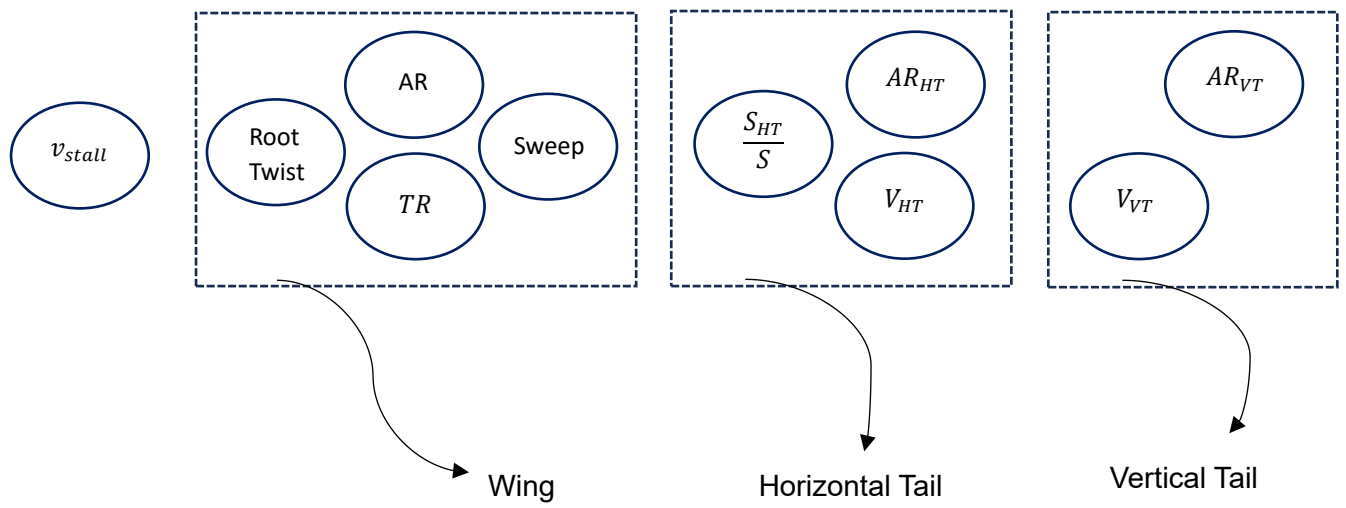
Decide: -



Estimate: -

Maximum Take Off Weight (MTOW)

Assume: -



4.2.2 Geometries Estimation

(1) Get Wing Area (S)

$$S = \frac{MTOW}{\frac{1}{2} * \rho * v_{stall}^2 * C_{l_{max}}}$$





(2) Get Wing Span (b) → $b = \sqrt{S * AR}$

(3) Get Wing Chord (C) → $C = \frac{b}{AR}$

(4) Get Wing Root Chord (C_r) → $C_r = 2 * \frac{S}{b * (1 + TR)}$

(5) Get Wing Tip Chord (C_t) → $C_t = TR * C_r$

(6) Get Mean Aerodynamic Chord (MAC) → $MAC = \frac{2}{3} * C_r * \frac{(1 + TR + TR^2)}{1 + TR}$

(7) Get Horizontal Tail Area (S_{HT}) → $S_{HT} = S * \frac{S_{HT}}{S}$

(8) Get Horizontal Tail Arm (L_{HT}) → $L_{HT} = \frac{V_H * S * MAC}{S_{HT}}$

(9) Get Horizontal Tail Span (b_{HT}) → $b_{HT} = \sqrt{AR_{HT} * S_{HT}}$

(10) Get Horizontal Tail Chord (C_{HT}) → $C_{HT} = \frac{b_{HT}}{AR_{HT}}$

(11) Get Vertical Tail Arm (L_{VT}) → $L_{VT} = L_{HT}$





(12) Get Vertical Tail Area (S_{VT})

$$S_{VT} = \frac{V_{VT} * S * b}{L_{VT}}$$

(13) Get Vertical Tail Span (b_{VT})

$$b_{VT} = \sqrt{AR_{VT} * S_{VT}}$$

(14) Get Vertical Tail Chord (C_{VT})

$$C_{VT} = \frac{b_{VT}}{AR_{VT}}$$

After using the procedure above and applying all the equations, now we have the necessary geometries of our RC plane to use an aerodynamic analysis software (XFLR5 in our case). Now the iterative process begins, we should try as much possible design points as we can till, we achieve a stable, suitable for our mission and satisfying design.

4.2.3 Drag Estimation

(1) Induced Drag (C_{d_i})

$$C_{d_i} = k * C_L^2$$

Where: - Oswald efficiency factor (e)

$$e = 0.8$$

$$k = \frac{1}{\pi * e * AR}$$

(2) Parasite Drag (C_{d_o}):-

$$C_{d_o} = 1.15 * \frac{C_f * FF * S_{wet}}{S}$$

Interference Drag





(a) Skin friction (assuming turbulent flow): -

$$C_f = \frac{0.455}{\log_{10} R_e^{2.58}}$$

(b) Form Factor: -

$$FF = FF_{fuselage} + FF_w + FF_{HT} + FF_{VT}$$

(1) Fuselage

$$FF_{fuselage} = 1 + \frac{60}{f^3} + \frac{f}{400}$$

Where f is slenderness ratio

$$f = \frac{L_{fuselage}}{\sqrt{\frac{4}{\pi} * A_{max,fuselage}}}$$

(2) Wing

$$FF_w = 1 + \left(0.6 * \frac{\left(\frac{t}{c}\right)_w}{\left(\frac{x}{c}\right)_{m_w}} \right) + \left(100 * \left(\frac{t}{c}\right)_w^4 \right)$$

(3) Horizontal Tail

$$FF_{HT} = 1 + \left(0.6 * \frac{\left(\frac{t}{c}\right)_{HT}}{\left(\frac{x}{c}\right)_{m_{HT}}} \right) + \left(100 * \left(\frac{t}{c}\right)_{HT}^4 \right)$$

(4) Vertical Tail

$$FF_{VT} = 1 + \left(0.6 * \frac{\left(\frac{t}{c}\right)_{VT}}{\left(\frac{x}{c}\right)_{m_{VT}}} \right) + \left(100 * \left(\frac{t}{c}\right)_{VT}^4 \right)$$

(c) Wetted Area: -

$$S_{wet} = S_{wet,fuselage} + S_{wet,w} + S_{wet,HT} + S_{wet,VT}$$

(1) Fuselage

$$S_{wet,fuselage} = 4 * Area_{rectangle}$$

Depending on
the fuselage
cross-section

(2) Wing

$$S_{wet,w} = 2 * \left(1 + \left(0.2 * \left(\frac{t}{c}\right)_w \right) \right) * S$$





(3) Horizontal Tail

$$S_{wet_{HT}} = 2 * \left(1 + \left(0.2 * \left(\frac{t}{c} \right)_{HT} \right) \right) * S_{HT}$$

(4) Vertical Tail

$$S_{wet_{VT}} = 2 * \left(1 + \left(0.2 * \left(\frac{t}{c} \right)_{HT} \right) \right) * S_{VT}$$

4.2.4 Thrust Estimation

4.2.4.1 Static Thrust

$$Thrust_{static} = MTOW * \left(\frac{(v_{lof}^2 - v_o^2)}{(2 * g * S_g)} + \left(q * \frac{C_{D_{To}}}{W/S} \right) + \mu \underbrace{\left(1 - q * \frac{C_{L_{To}}}{W/S} \right)}_{\text{Neglected because the plane is hand launched}} \right)$$

Neglected because the plane is hand launched

4.2.4.2 Dynamic Thrust at cruise

$$Thrust_{dynamic_{cruise}} = MTOW * \left(\frac{\left(\frac{1}{2} * \rho * v_{cruise}^2 * C_{d_o} \right)}{\frac{W}{S}} + \frac{\left(2 * k * \frac{W}{S} \right)}{\rho * \sigma * v_{cruise}^2} \right)$$

4.2.4.3 Dynamic Thrust at maximum speed

$$Thrust_{dynamic_{max}} = MTOW * \left(\frac{\left(\frac{1}{2} * \rho * v_{max}^2 * C_{d_o} \right)}{\frac{W}{S}} + \frac{\left(2 * k * \frac{W}{S} \right)}{\rho * \sigma * v_{max}^2} \right)$$

Where: -

(a) Lift off speed (v_{lof})

$$v_{lof} = (1.1 \text{ to } 1.3) * v_{stall}$$





(b) Hand launching speed (v_o)

$$v_o = 5$$

(c) Gravitational acceleration (g)

$$g = 9.81$$

(d) Ground run (S_g)

$$S_g = 5$$

(e) Dynamic pressure (q)

$$q = \frac{1}{2} * \rho * \left(\frac{v_{lof} - v_o}{\sqrt{2}} \right)^2$$

(f) Drag Coefficient during T-O run ($C_{D_{To}}$)

$$C_{D_{To}} = C_{d_o} + (k * C_{L_{max}}^2)$$

(g) Ground friction constant (μ)

$$\mu = 0$$





4.3 Idesign (Graphical User Interface Program)

4.3.1 Program Function

This program is made to help the user through the process of designing of remote-controlled plane by: -

1. Calculating the geometries for a chosen design point.
2. Estimation for the Thrust and the Drag.
3. Performance analysis of the plane.

Notes: -

1. An aerodynamic analysis program like (XFLR5) maybe needed to provide some inputs.
2. The assumptions this program based on, are provided in a text within the program file

4.3.2 Calculating Geometries

In order for the program to calculate the geometry of the plane the inputs below are required from the user.

4.3.2.1 Program Inputs

Related To the Aircraft

1. Maximum take-off weight of the plane.
2. Stall speed.

Related To the Altitude

3. The Design altitude.
4. Cross-pounding kinematic viscosity.

Related To the Vertical Tail

5. Volumetric Ratio
6. Aspect Ratio

Related To the Horizontal Tail

7. Area Ratio
8. Volumetric Ratio
9. Aspect Ratio

Related To the Wing

10. Aspect Ratio
11. Maximum lift Coefficient
12. Taper Ratio





4.3.2.2 Outputs

As soon as the user provide the program with the inputs with the correct units, the program can now process and give the user the outputs which are: -

Related To the Wing

1. Area
2. Span
3. Chord
4. Root Chord
5. Tip Chord
6. Mean Aerodynamic Chord

Related To the Horizontal

7. Area
8. Span
9. Chord
10. Arm

Related To the Vertical Tail

11. Area
12. Span
13. Chord
14. Arm

4.3.3 Estimating Thrust and Drag

For the design point cross-pounding to the user inputs, the program can now save the need parameters and ask the user for further more inputs so it can estimate the drag and the thrust of the plane.

4.3.3.1 Program Inputs

Related To the Fuselage

1. Length
2. Maximum Area

Related To the Vertical Tail

1. Chordwise Location of The Airfoil Maximum Thickness Point (%)
2. Airfoil Maximum Thickness Point Location to Chord (%)

Related To the Horizontal Tail

3. Chordwise Location of The Airfoil Maximum Thickness Point (%)
4. Airfoil Maximum Thickness Point Location to Chord (%)

Related To the Wing

5. Chordwise Location of The Airfoil Maximum Thickness Point (%)





-
6. Airfoil Maximum Thickness Point Location to Chord (%)

Other Important Parameters

7. Reynolds Number
8. Lift Coefficient
9. Oswald Efficiency (%)

4.3.3.2 Program Outputs

the program can now process and give the user the outputs which are: -

Drag

1. Induced Drag coefficient
2. Parasite Drag coefficient
3. Total Drag

Thrust

4. Static Thrust
5. Dynamic Thrust at cruise speed
6. Dynamic Thrust at maximum speed

4.3.4 Performance Calculations

In order for the user to have a note about the design point and how the plane with these characteristics can perform, some performance parameters can be calculated.

4.3.4.1 Inputs

1. Altitude to test the plane at
2. Motor power
3. Propeller efficiency
4. Battery ampere
5. Battery voltage

4.3.4.2 Outputs

1. Maximum Velocity
2. Minimum Velocity
3. Maximum rate of climb
4. Velocity for maximum rate of climb
5. Minimum Thrust
6. Velocity for minimum thrust
7. Minimum Power required
8. Velocity for minimum power
9. Maximum Range
10. Maximum Endurance





4.3.5 Program Simulation



Figure 5-Geometry Tab Interface

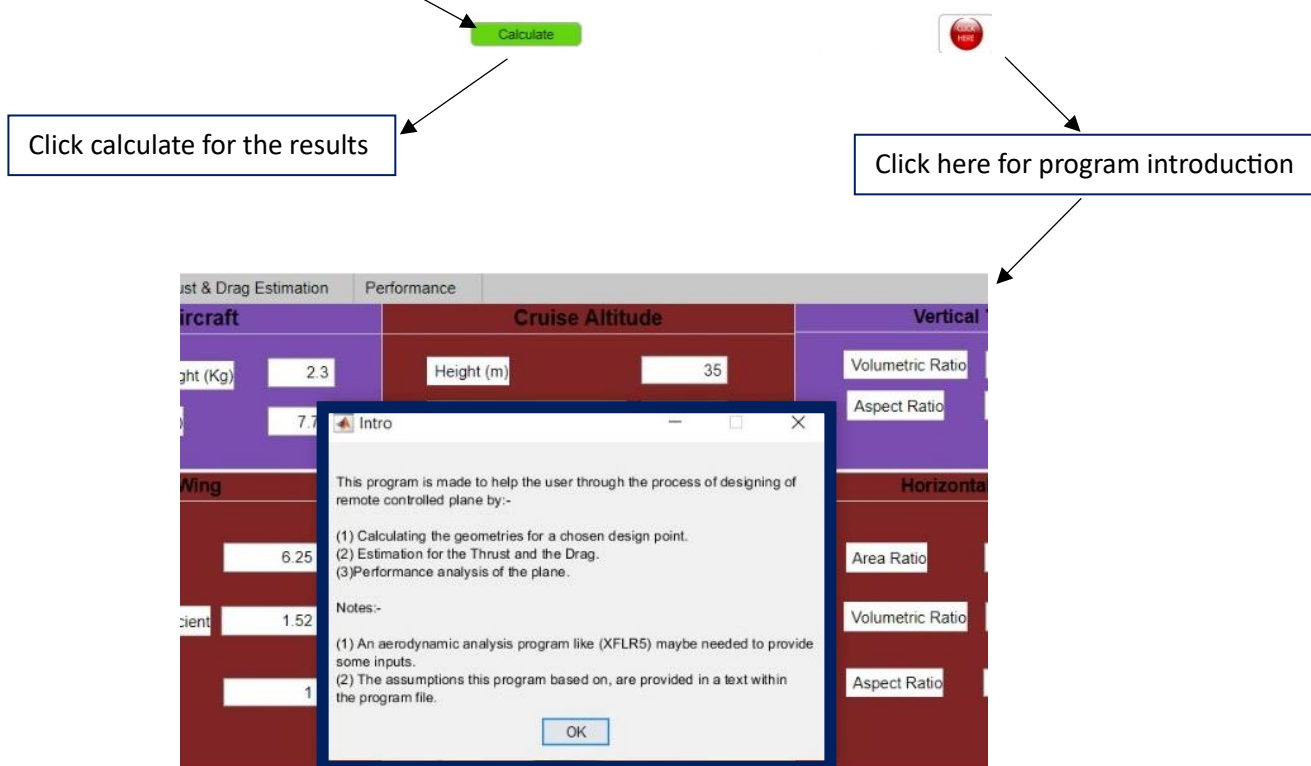


Figure 6-Program Instructions



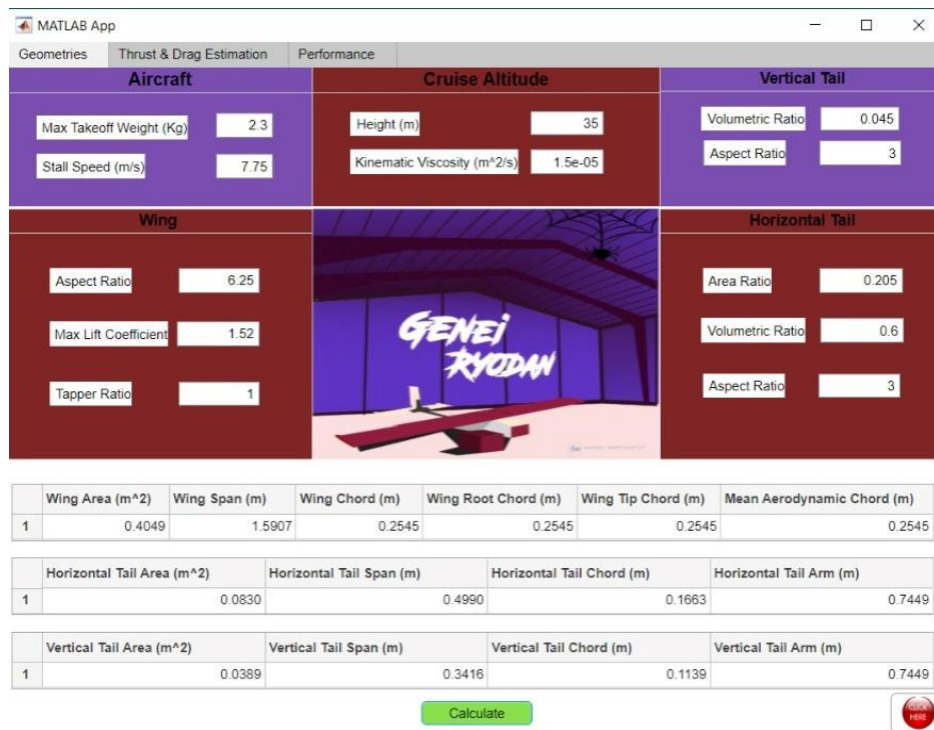


Figure 7-Geometery Results



Figure 8- Thrust and Drag Tab Interface



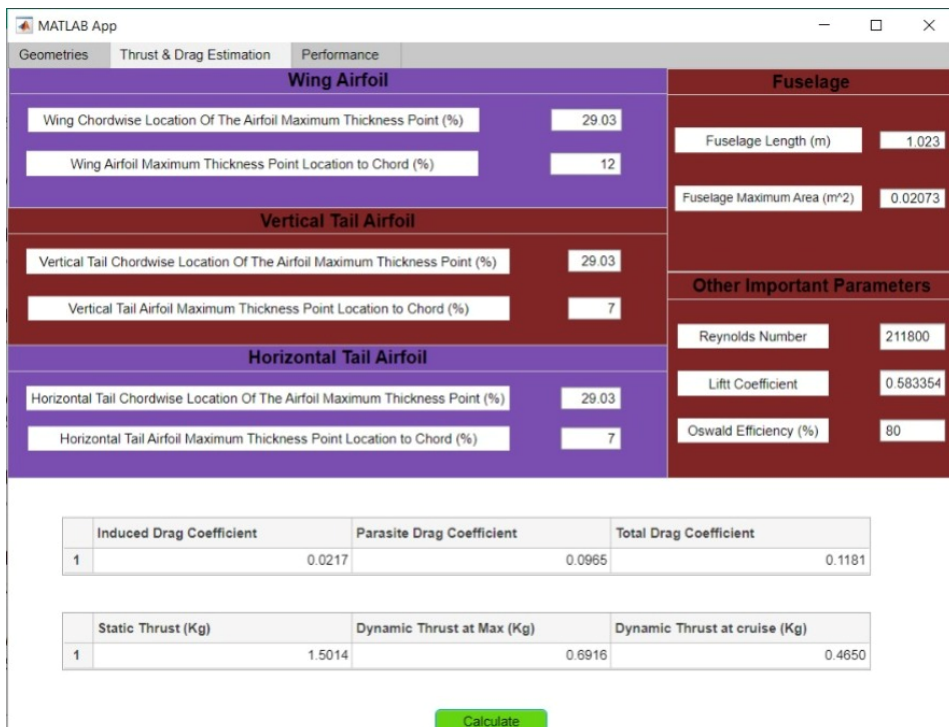


Figure 9- Thrust and Drag Results

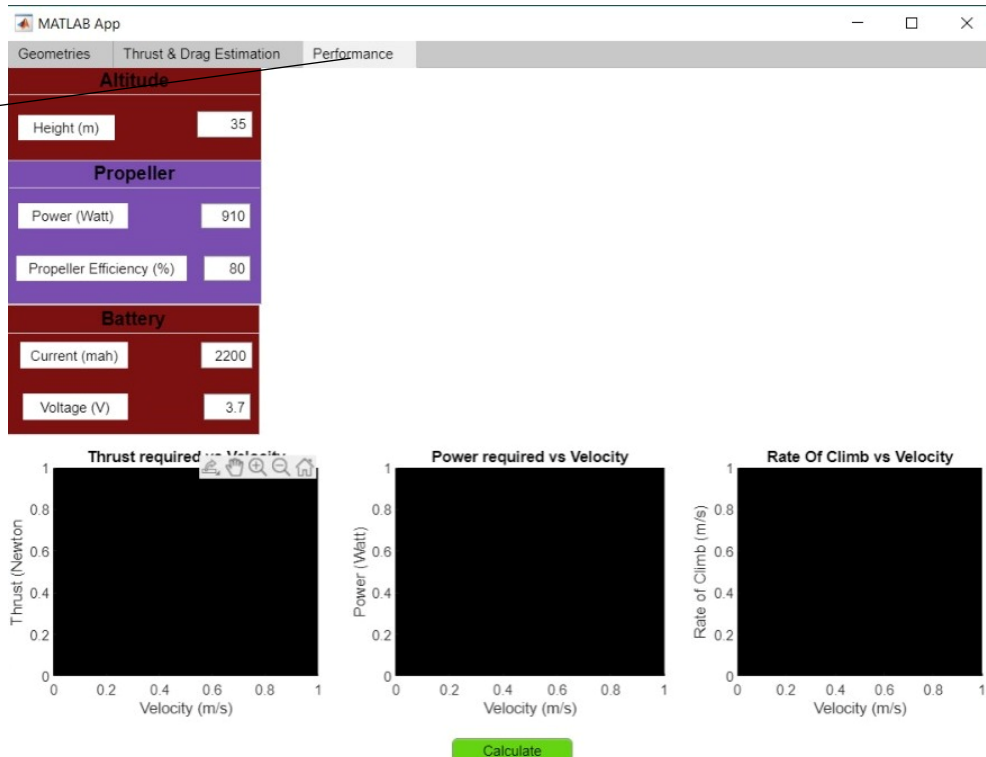


Figure 10- Performance Tab Interface



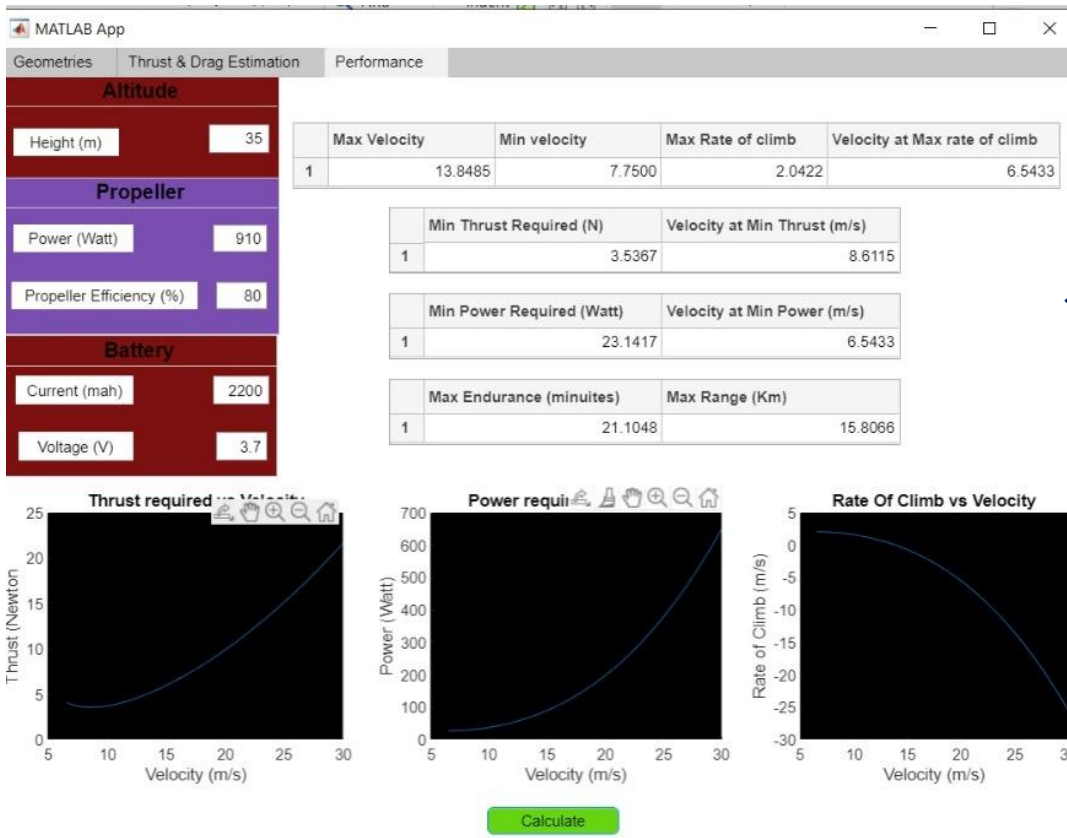


Figure 11- Performance Results

4.4 Design and Sizing Trade Studies

4.4.1 Fuselage Design and Sizing

The primary parameter in fuselage sizing and design is weight. The fuselage was initially sized to have the smallest possible cross-section. The fuselage consists of two sections, the rear section is designed to hold the payload, and the front section contains the avionics compartment. The main fuselage, consisted of the motor, avionics, payload bay, and tail interface, was sized to transfer all primary loads from the motor, wings, and tail interface. The tail section, which consisted of the tail boom and tail connector, was sized to enable the transfer of all loads from the empennage to the main fuselage. The internal structure of the fuselage consists of two sides connected together by bulkheads and motor mount. The side, motor mount and bulkheads are made of plywood with 3mm thickness the sides are made in the form of a truss to reduce as much weight as possible. The cross-sectional shape was selected to be a filleted rectangle, as this had minimal impact on drag compared to a circle, was easier to manufacture and interface with other aircraft components. The total length of the fuselage was determined to be



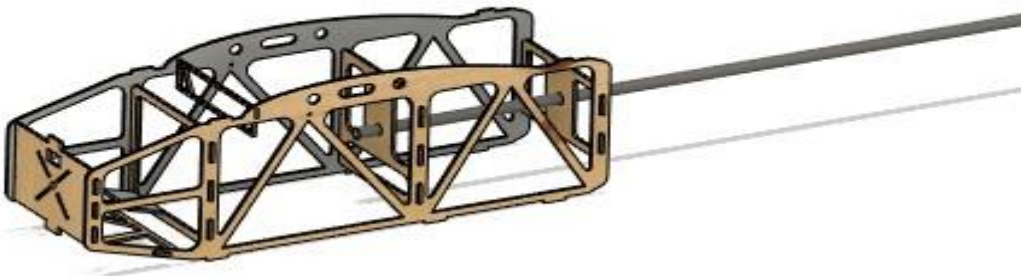


Figure 12-Fuselage Sizing

4.4.2 Airfoil Selection

The airfoil selection was the first step in aerodynamic sub-system, after the mission had been sent by the coordinators of the competition we had started to search in the specifications of this mission, it's constraints and how to achieve the best results. We had reached to good point that we need an airfoil with high lift coefficient at the desired range of Reynold's number which is between 50 and 300 thousand so we can get a high payload weight to aircraft weight ratio which is an important factor of scoring. Each one in the aerodynamic team had started to search to get the desired airfoil which has high lift coefficient and at the same time it undergoes to the constraint of maximum and minimum thickness of the airfoil so we can manufacture easily with no problems. The following table shows the best airfoils for our mission and the selected one.

Figure of merit	Factor	NACA 2412	Clark Y	Eppler 205	FX 63-137	CH 10-48-13	M06-13-128	SG6042	S1210
c_{L_0}	0.2	2	3	2	1	2	2	3	3
$c_{L_{Max}}$	0.2	3	3	2	2	3	3	3	3
C_D	0.2	1	2	2	2	1	2	2	1
$\frac{C_L}{C_D}$	0.2	1	2	2	2	3	3	2	3
Manufacturing	0.2	3	2	2	3	2	1	3	1
Total Score	1	2	2.4	2	2	2.2	2.2	2.6	2.2

Table 9- Airfoil Selection Decision Matrix





And this is a sample how we can get all the specifications of any airfoil through XFLR5 (The following specifications belongs to the chosen airfoil which is SG6042).

1. From airfoil tools website or any other source, we can get the x and y points which draw the airfoil in format of file.dat
2. We insert the file in XFLR5
3. From module choose xfoil direct analysis
4. From analysis choose batch analysis and put the desired range of Reynold's number, minimum and maximum angle of attack and the increment.
5. You can get any graph by simply choose the variables on the y and x axes.
6. Putting alpha on the x axis and C_l or C_d and $\frac{C_l}{C_d}$ on the y axis you can get the required specifications

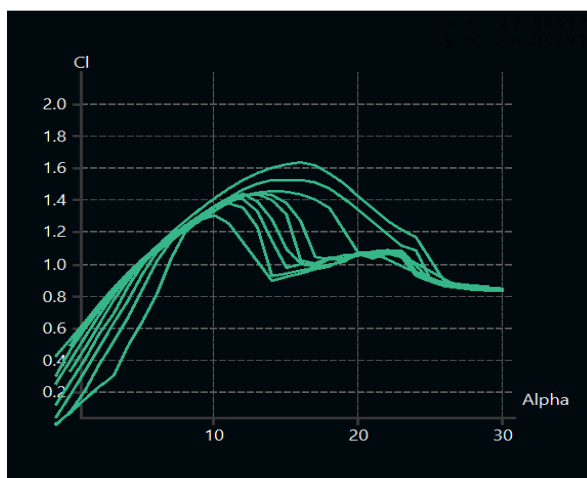


Figure 13- Airfoil's C_l versus α curves at different Reynold's number

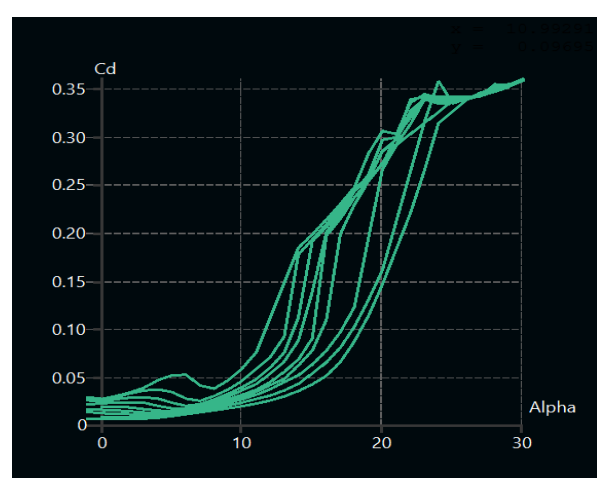


Figure 14-Airfoil's C_d versus α curves at different Reynold's number

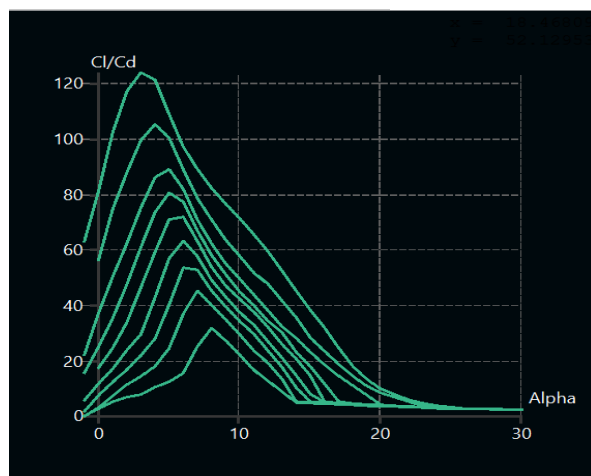


Figure 15- Airfoils C_l/C_d versus α curves at different Reynold's number





4.4.2 Wing Design and Sizing

The primary goal of wing sizing and design is to maximize the wing's lift with a secondary goal of reducing its drag while in cruise. The lift a wing can generate is directly proportional to its reference area (S), airspeed (V), air density (ρ), and its lift coefficient (CL) as shown in Equation (1)

$$L = \left(\frac{1}{2}\right) * \rho * V_{stall}^2 * S * CL_{stall} \quad (1)$$

Increasing the wing area will increase the MTOW and wing lift of the aircraft, so the MTOW of 2300 Kg was chosen and the wing area ($0.403m^2$) was calculated by using MTOW (2300), the stall speed (7.75 m/s), and the maximum lift coefficient (1.52) as shown in Equation (2). The wing span and wing chord was determined using aspect ratio (6.25), Taper ratio (1), by using Equations (3), (4)

$$W = \frac{1}{2} * \rho * V_{stall}^2 * S * CL_{max} \quad (2)$$

$$b^2 = (AR * S) \quad (3)$$

$$Cr = \frac{2 * s}{b(1 + \lambda)} \quad (4)$$

A rectangular wing was chosen for its ease to manufacture. No wing twist or dihedral are used, as they are difficult to manufacture. But the winglet was added to improve lateral stability. The resulting design provided a balance between maximizing wing area, flight stability and ease of manufacture. Therefore, the wing sizing process resulted in a simple but effective process, as summarized in Table1

parameter	Span (m)	Area (m^2)	Aspect Ratio	Taper Ratio	Dihedral (deg)	Twist (deg)	Mac (m)
value	1.587	0.403	6.25	1	0	0	0.254

Table 10- Wing Parameters

4.4.3 Tail Design and Sizing

In sizing the vertical and horizontal stabilizers, volume coefficient of 0.045 and 0.6, respectively and horizontal tail -to-wing area ratio of 0.205, were chosen, Surface area was determined using wing area ($403.08 mm^2$), and horizontal tail arm was determined using wingspan (158.72 mm), wing aerodynamic chord (253.96 mm), For the vertical tail, the resulting dimensions were 340.89 mm of span, and 113.63 mm at maximum chord. The corresponding dimensions for the horizontal tail were 497.89 mm of span and 165.965 mm of chord.





4.4.3.1 Horizontal Tail

Parameter	Volumetric Ratio	Area Ratio	Span (m)	Chord (m)	Area (m^2)	Aspect Ratio	Incident angle (deg)	Arm
Value	0.6	0.205	0.498	0.166	0.083	3	-2.5	0.743

Table 11- Horizontal Tail Parameters

4.4.3.2 Vertical Tail

Parameter	Volumetric Ratio	Span (m)	Chord (m)	Area (m^2)	Aspect Ratio	Incident angle (deg)	Arm
Value	0.045	0.341	0.114	0.039	3	-2.5	0.743

Table 12- Vertical Tail Parameters

4.4.5 Control surface Design and sizing

The goal of control surface sizing is to ensure that the aircraft is both manoeuvrable and controllable. The elevator, rudder, and ailerons are sized to provide sufficient control in the longitudinal, vertical, and lateral axes, respectively

4.4.5.1 Rudder

Parameter	Span (m)	Chord (m)	Area (m^2)
Value	0.328	0.029	0.007

Table 13- Rudder parameters

4.4.5.2 Elevator

Parameter	Span (m)	Chord (m)	Area (m^2)
Value	0.447	0.042	0.0186

Table 14- Elevator Parameters

4.4.5.3 Aileron

Parameter	Span (m)	Chord (m)	Area (m^2)
Value	0.277	0.085	0.0193

Table 15- Aileron parameters





4.4.6 Parachute Sizing

In order to calculate the area of the parachute needed to carry the payload and provide landing terminal velocity less than the velocity which trigger the 25G shock sensor.

The following formula is used to calculate the area.

$$Area_{parachute} = \frac{2 * g * m_{total}}{\rho * C_d * v_{terminal}^2}$$

Where: -

1. g is the gravity acceleration
2. m_{total} is the mass of the payload and the parachute which = 0.9 Kg in our case
3. ρ is the air density which is 1.225
4. C_d is the drag coefficient estimated by 0.75 for round canopy
5. $V_{terminal} = 4.5 \text{ m/sec}$

Based on some research we had determined the value of the terminal velocity that would be logical to our mission. Based on omni calculator and it's a calculator that you can do on it the calculations easily by putting the inputs mass, cross-sectional area of the parachute, the coefficient drag, density of the fluid and acceleration due to gravity and all these inputs are constants based on our configurations and the mission environment and the output will be the terminal velocity. Our objective was to decrease the terminal velocity as possible to maintain our shock sensor not triggered. So firstly, we decided the terminal velocity to be 2m/s and we waited the program to give us the area of the parachute as an output instead of terminal velocity as an output and it was 4.8 m^2 which means parachute of diameter 2 m and this is a huge parachute and not reasonable to obtain for this mission so we have decided to double the terminal velocity so the parachute will be halved.

from the calculations above we found that we need a parachute with an Area = 0.948 m^2

for round canopy the diameter is found by the formula $D = \sqrt{\frac{4*s}{\pi}}$ which is leading to diameter of 109.8 cm \cong 110 cm which is reasonable diameter area for this mission. Beside determining the diameter of the parachute there is also a spill hole that should be made in the middle of the parachute according to out parachute's final design configuration and also determining the length of the parachute robes that will hold the box. According to some researches we had found that the best ratio for the diameter of the spill hole to be 20% of the diameter of the parachute, which means a spill hole of diameter 22 cm should be made in the middle of the parachute and the

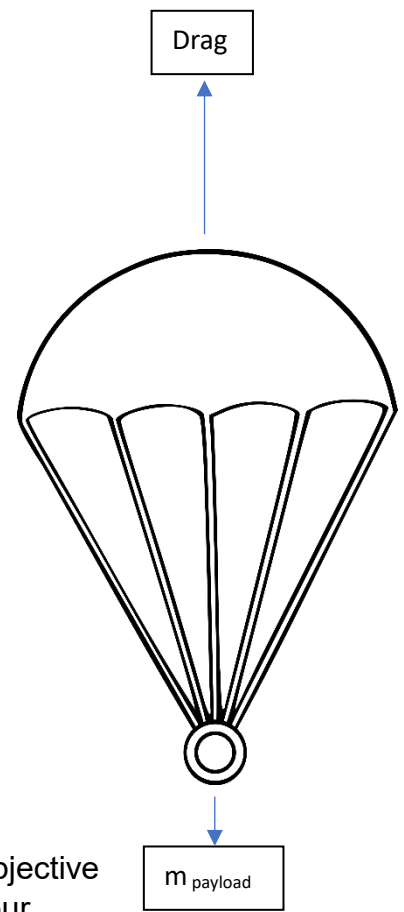


Figure 16- Forces affecting the Parachute





length of the shroud that will hold the box should be 1.15 the diameter of the parachute, which means a shroud of length 126.5 cm.

4.4.7 Propulsion Sizing

Our propulsion system consists of a battery, an ESC (electronic speed controller), a brushless motor, and a propeller. We had a few options to choose from for each component so we kept trying different combinations to see which will most satisfy the mission requirements.

1. Battery options: HRB 5200mAh or LiPo 2200mAh
2. ESC options: eflight Max Current either 30A or 60A
3. Motor options: Electrify 1200Kv, Emax 1400/1800Kv, or Turnigy 11000Kv
4. Propeller options: APC SlowFly 12,11, or 10-inch diameter

We faced a challenge when choosing the set at the beginning because it had a very good performance but was also very heavy. After a few more trials, we reached the optimum set for our UAV. The following figure shows more details on the performance of the propulsion sizing in terms of static and dynamic thrust, temperature, efficiency, and endurance.



Figure 17- Propulsion Sizing Performance on eCalc

4.5 Aircraft Stability Analysis

The stability was analysed using XFLR5. Once the base aircraft dimensions were defined, a model was created in XFLR5. All static stability derivatives were determined to be within an acceptable range, as discussed in the stability sessions. Additionally, flight test analysis and pilot feedback further validated the stability.

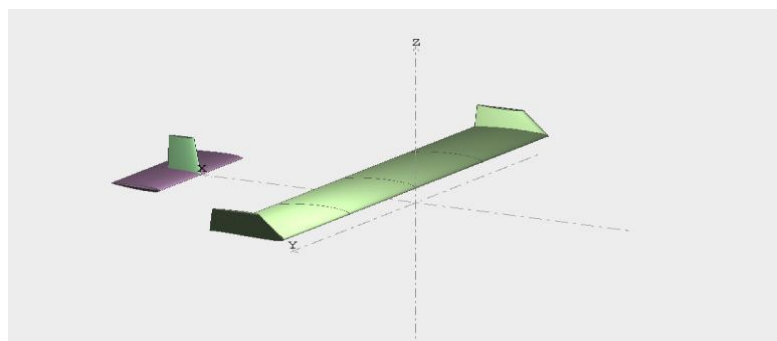


Figure 18- Aerodynamic Configuration on XFLR5





4.5.1 Static Stability

To ensure the static stability of the aircraft in all missions, we decided that the payload will be in the place of CG beside that we set the CG according to XFLR5 which was 8.6 cm from the leading edge of the wing, so this is the CG position during the whole flight. The electronics package mounting location was chosen such that its position put the CG of the whole aircraft as stated in XLRF5. The neutral point was determined by XFLR5 at 12.6 cm from the leading edge and this is behind the CG to ensure the static stability of the aircraft, after putting the static margin by 15.75% to make sure that the aircraft will not be over stable and can do some maneuvers the CG position had been determined. The aircraft's stability derivatives were calculated in. All values possess the correct signs to indicate stable flight behaviour. This analysis was performed to ensure that the curves show that the aircraft is stable longitudinally, directionally and laterally. To ensure that the aircraft is longitudinally stable a negative incidence angle for horizontal stabilizer is required, after searching this angle was in range between 1 to 3 degrees our choice was based after more than one analysis to ensure better longitudinal stability for our aircraft and the choice has been set to 2.5 degrees. The following figure shows our model on XLRF5 after setting the geometry of wing, horizontal stabilizer and vertical stabilizer. Then defining an analysis choosing reference dimension wing planform projected on xy plane in all types of analysis. With polar type 2 (fixed lift), ring vortex analysis setting our plane mass (2.3kg), XCG, ZCG and setting the start, end and increment of alpha. The following graphs shows the static stability of our airplane and some important specifications as trim angle it is 2.1 degrees and cruise speed which is 16 m/s.

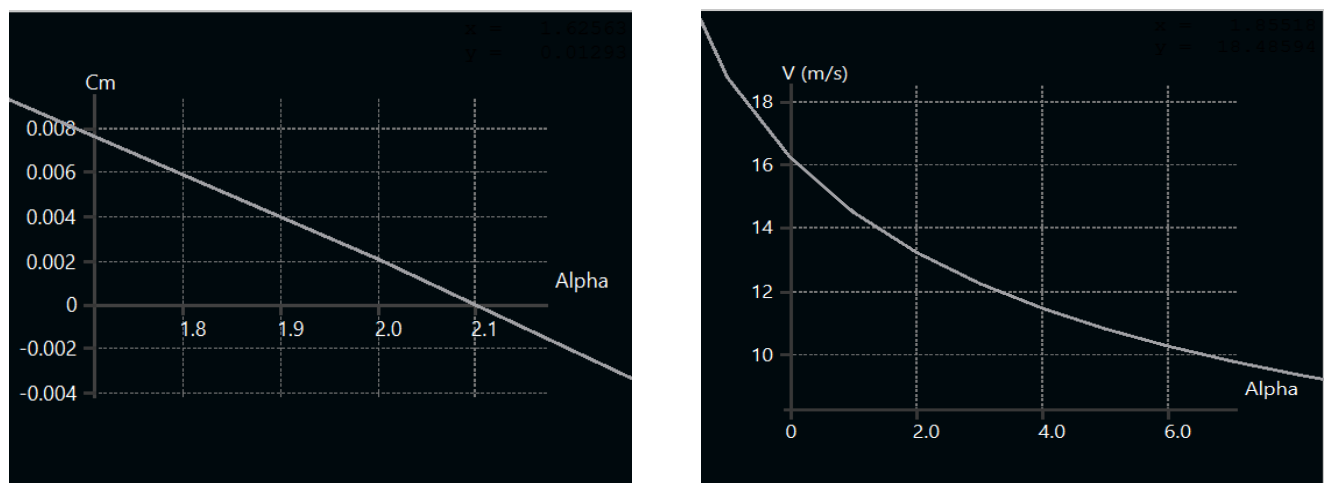


Figure 19-C_m and V Versus Alpha Curves of M1





The next step was to determine the directional and lateral stability and ensure that our aircraft is directionally and laterally stable and this was through choosing polar type 5 (beta range) and setting the cruise speed (16 m/s) and trim angle (2.1 degrees) and choosing ring vortex analysis as this analysis including the sideslip angle.

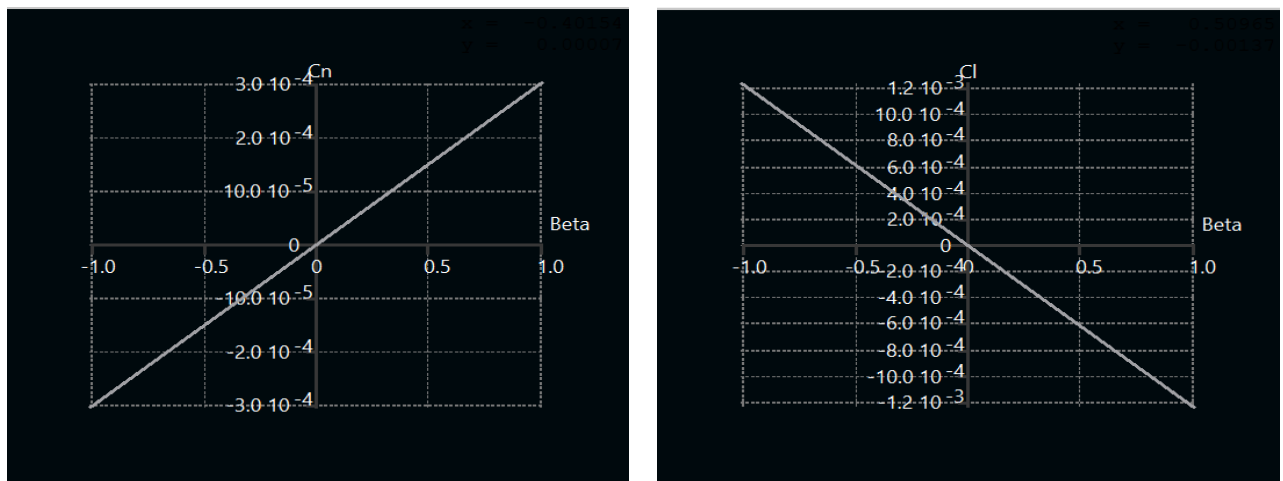


Figure 20- C_n and C_l versus Beta curves of M1

Same steps are done for the aircraft to ensure its static stability but this time after dropping its payload, the total weight will be dropped to 1.4kg instead of 2.3kg which means the payload estimated weight is 0.9 kg with no any change in XCG as the payload will be at the same point as mentioned before so there is no change before loading or dropping the cargo, the trim angle remained the same but there was change in cruise speed it is dropped to 12.6 m/s.

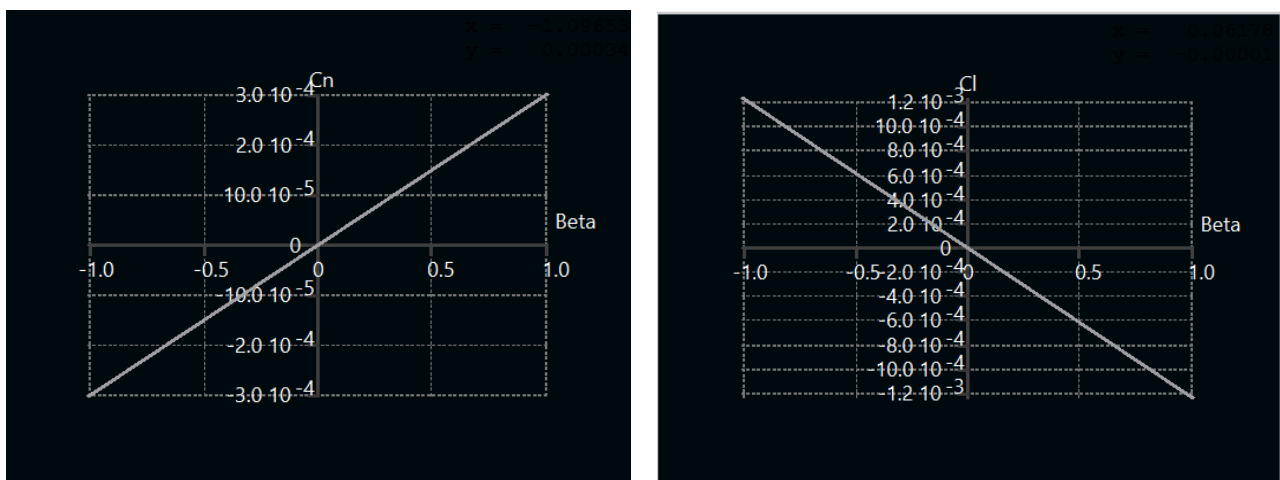


Figure 21- C_n and C_l versus Beta curves of M2



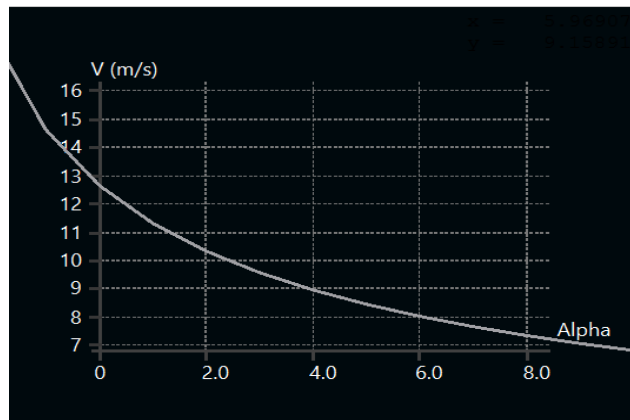


Figure 22- V Versus Alpha Curve of M2

4.5.2 Dynamic Stability

XFLR5 was used to determine the pole placement of both longitudinal and lateral modes of the aircraft with and without the payload to ensure that the aircraft will be dynamically stable along the whole flight, the analysis is made to ensure that the longitudinal poles (two for short period mode and two for long period mode) the poles of short period mode is found far away from the imaginary axis while the long period mode is found nearest the imaginary axis, the short period mode is named like this because when disturbance occurs it settles in short period while long period mode or phugoid mode is named like this because when disturbance occurs it settles in more time. The following graphs shows the longitudinal and lateral pole placement of the aircraft loaded with the payload. All poles lie on the left-hand side and to determine the level of the flight which means to see how much stable the aircraft is, we had used UDC-dynamic stability assessment tool using Damping ratio which is symbolized ζ , damped natural frequency which is symbolized w_d which is symbolized as F_1 , time to double which is symbolized as T_2 or t_2 on XFLR5 and time constant which is symbolized as τ .

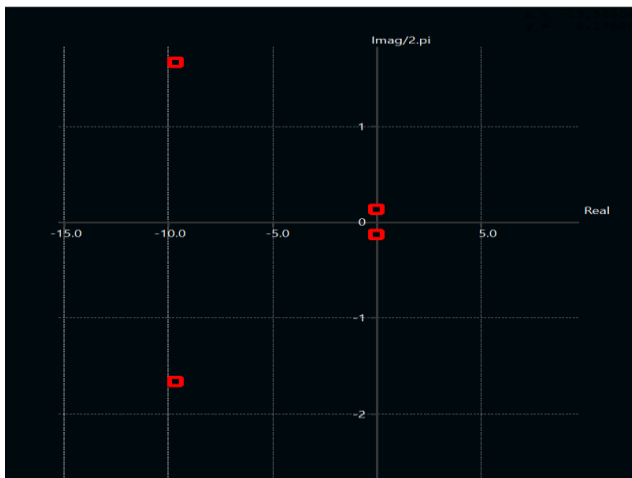


Figure 23-Longitudinal Pole Displacement of M1

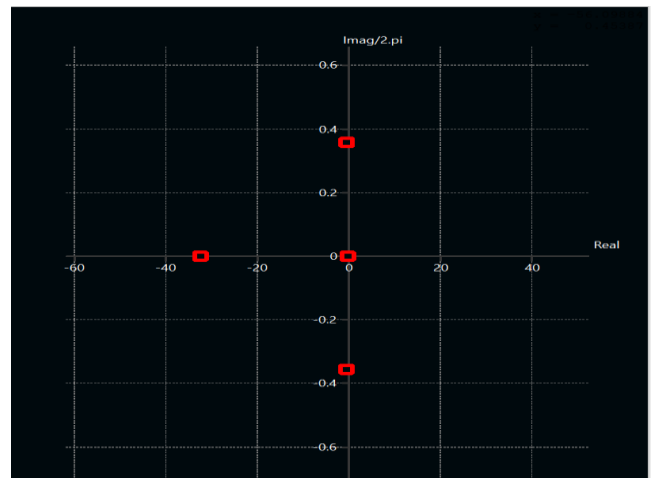


Figure 24-Lateral Pole Displacement of M1





Modes		ζ	w_d	T_2	τ
Longitudinal	Short Period	0.67			
	Phugoid	0.0077			
Lateral	Roll				0.03
	Dutch	0.144	0.355		
	Spiral			617	

Table 16- Aircraft Stability Parameters of M1



Figure 25- Flight Level Indicators

XLRF5 is also used to determine important specifications of the aircraft's mode one of these important specifications is to simulate the response of the aircraft's modes, for verifications, longitudinal modes of the aircraft are affected by some parameters which are longitudinal speed, vertical speed, pitch rate and pitch angle which have the symbols u , w , q and θ respectively. w and q affect the short period mode mostly while u and θ affect the long period mode mostly. We are interested to see the settling time and damping simulation of these parameters to ensure that the aircraft will stabilize itself as we will see in the following graphs that w and q which affect the short period mode have high damping in the beginning but they settle very fast almost after 0.8 second while u and θ which affect the long period mode have very low damping response but they settle in much more time which is 500 second.

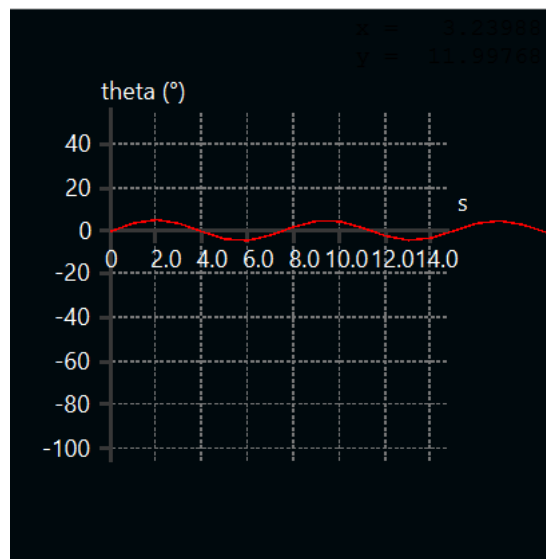
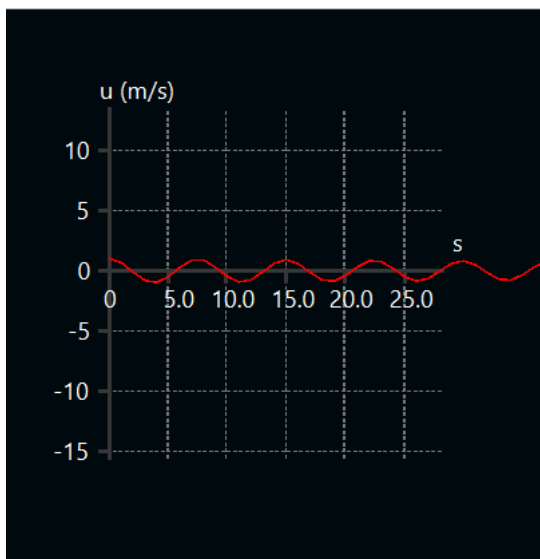


Figure 26- Longitudinal Velocity and Pitch angle Simulation of Phugoid Mode



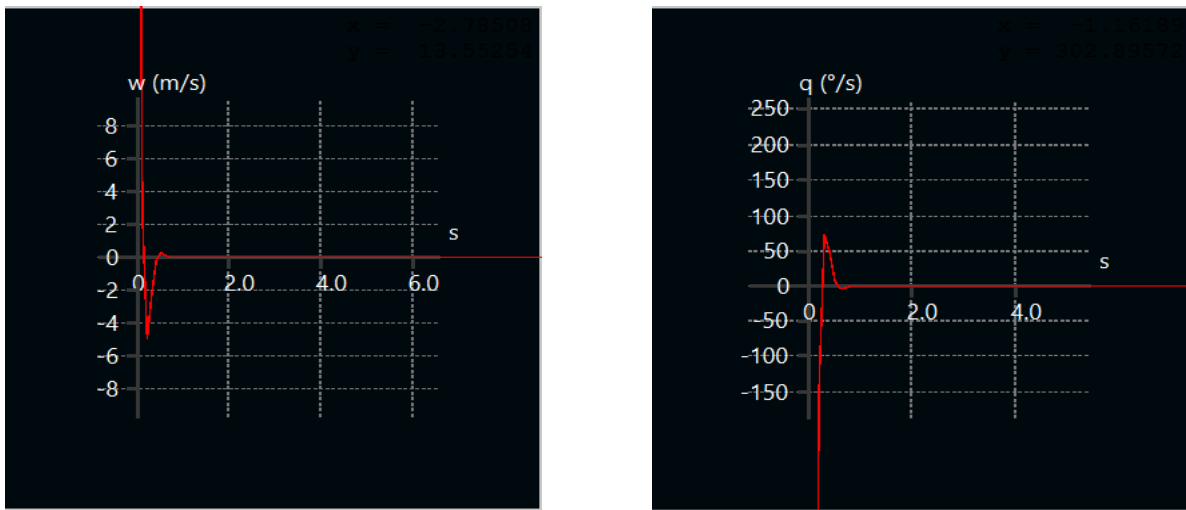


Figure 27- Vertical Velocity and Pitch rate Simulation of short period mode

Lateral modes of the aircraft are affected by some parameters which are side velocity, roll rate, yaw rate and roll angle which have the symbols v , p , r and φ respectively. v and r affect the dutch mode mostly, p affect the roll mode mostly and r affect the spiral mode mostly. We are interested to see the settling time and damping simulation of these parameters to ensure that the aircraft will stabilize itself as we will see in the following graphs that v and r which affect the dutch mode have low damping for v and very low damping for r and settles after 10 seconds, p which affect roll mode have high damping response in the beginning but it settle after 0.4 which is very fast second and r which affect the spiral mode has very low damping but settles after very long time which makes it dangerous on the airplane.

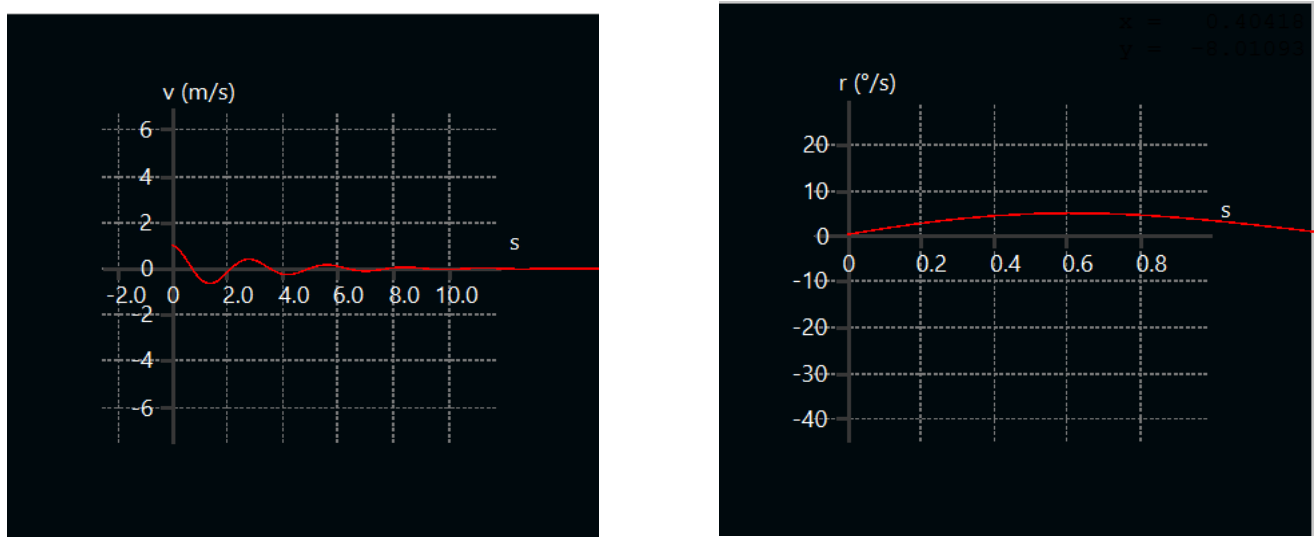


Figure 28- Side Velocity and Yaw rate of dutch mode simulation



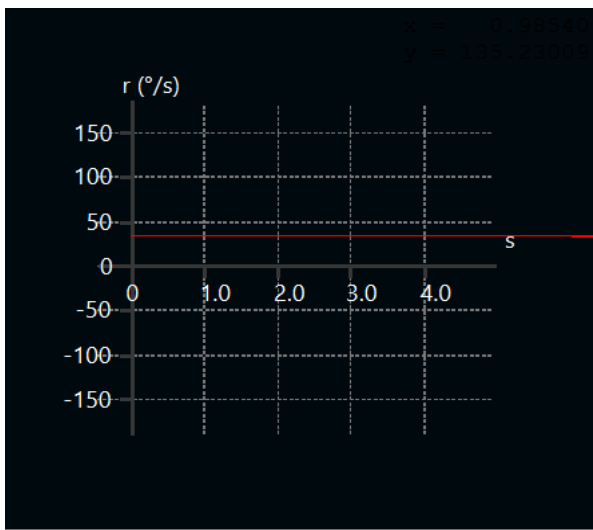


Figure 29-Yaw rate Simulation of Spiral Mode

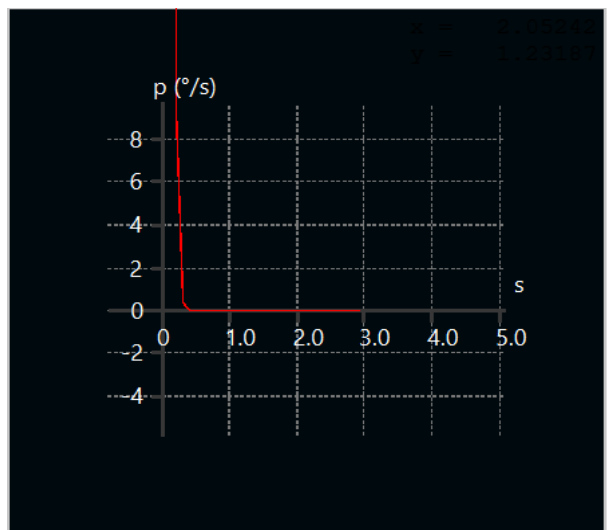


Figure 30- Roll rate Simulation of Roll Mode

The same steps are done to the aircraft after dropping the cargo which means the aircraft's weight is 1.4kg and the figure of pole placement also ensures that the aircraft after dropping the cargo has all the poles lie in the left-hand side and also using the UDC-dynamic stability assessment tool we have ensured that the flight level is good.

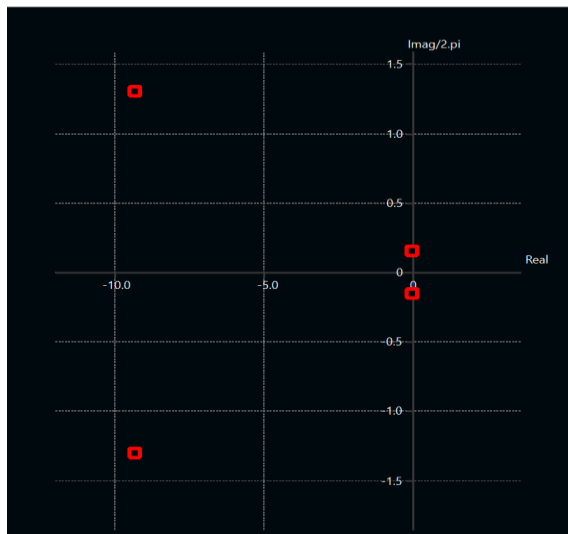


Figure 31-Longitudinal Pole Displacement of M2

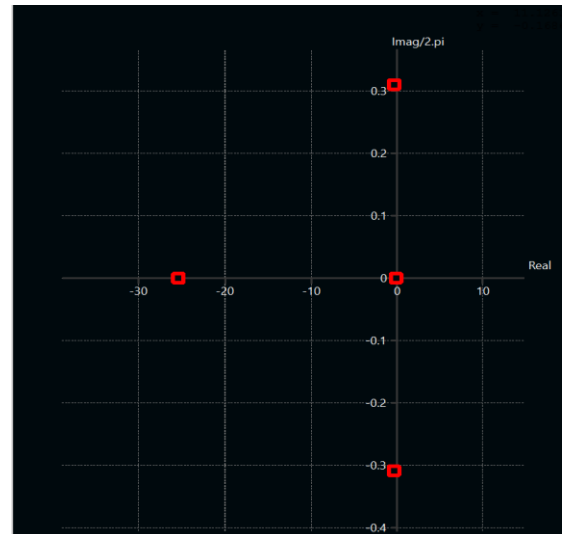


Figure 32-Lateral Pole Displacement of M2





Modes		ζ	w_d	T_2	τ
Longitudinal	Short Period	0.75			
	Phugoid	0.0028			
Lateral	Roll			0.04	
	Dutch	0.155	0.3		
	Spiral	600			

Table 17- Stability parameters of M2



Figure 33-Flight Levels Indicators

The same simulation figures had been done by XFLR5 to ensure that the damping and settling time of parameters that affect short period, long period, roll, dutch and spiral modes are accepted and there is no difference in the damping and settling time between the aircraft with payload and without payload.

5.0 Detailed Design

The detailed design phase uses what was learned and selected During trade studies and preliminary design to optimize the aircraft for performance and functionality.

5.1 Dimensional parameters

The next table shows the dimension of each component in each subsystem.

Wing		Horizontal Stabilizer		Propulsion	
Airfoil	SG6042	Airfoil	Flat plate	Motor	Turnigy
Span	1587 mm	Span	497.8 mm	Motor rated kv	1100
MAC	254 mm	Chord	154.9 mm	Motor weight	165 g
Wing Area	403088 mm ²	AR	3	propeller	APC-SlowFly SF
Root Chord	254 mm	Area	82600 mm ²	Battery	Lipo
Tip Chord	254 mm	Angle of Incidence	-2.5	Battery's capacity	2200
Taper Ratio	1	Fuselage		Max discharge rating	35C
Leading edge sweep	0 deg	Total length	470.5mm	Weight	62.5*4 g
Angle of incidence	0 deg	Tapered nose section Length	101mm	ESC	
Static Margin	16.5%	Nose maximum height	140mm	Model	Max 60 A
Vertical Stabilizer		Midsection straight length	351mm	Resistance	0.0045 ohm





Airfoil	Flat plate	Midsection maximum height	150mm	mass	20 g
Height	340.8 mm	Midsection minimum height	140mm	Controls	
Root Chord	120 mm	Backward length	17.2mm	Transmitter	Spektrum DX8
Tip Chord	88 mm	Backward maximum height	140mm	Receiver	Spektrum 6 channel AR620
Area	38714 mm^2	Backward minimum height	111mm	Wing Servos	SG90
AR	3	Length of boom in fuselage	187.4mm	Elevator and rudder servos	SG90
Leading edge sweep	0 deg	Corners filler radius	10mm	Mechanism Servos	SG90

Table 18- Dimensional Parameters

5.2 Subsystem Design

5.2.1 Fuselage Skin

1. The skin of the fuselage is made of white foam and flattened to become one piece. Making it into one piece leaves no room for discontinuity in the overall structure and therefore supports the smoothness of airflow around it. The skin also has holes that the bulkheads will get fixed into.
2. The mechanism used to drop the payload is also attached to the skin from the outside of the UAV. Using a servo, a small iron stick will be unlocked and the rubber band will let loose and drop the payload.

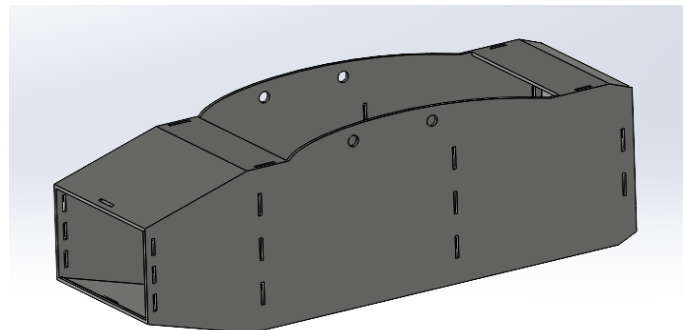


Figure 34- Skin Subsystem

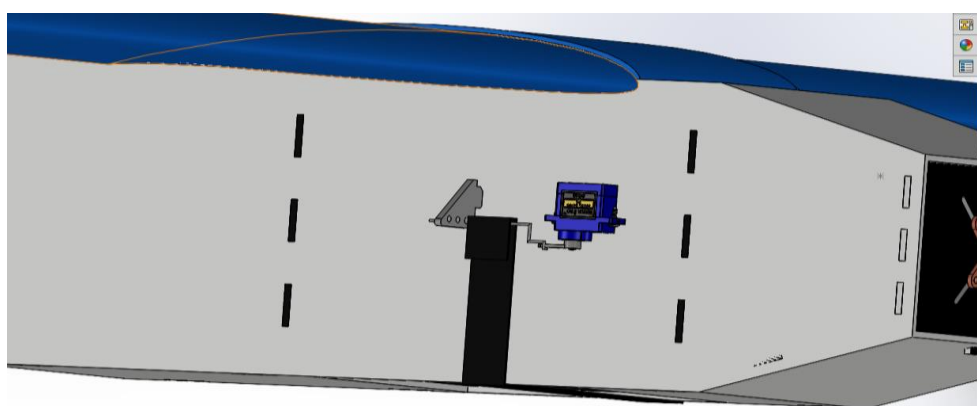


Figure 35-Payload Dropping Mechanism





5.2.2 Internal Structures

1. The internal structure of our UAV is made of plywood and designed in the form of trusses to reduce structural weight and distribute stress as equally as possible along it.
2. The bulkheads were also made out of plywood and were designed to fit the boom exactly with no tolerance.

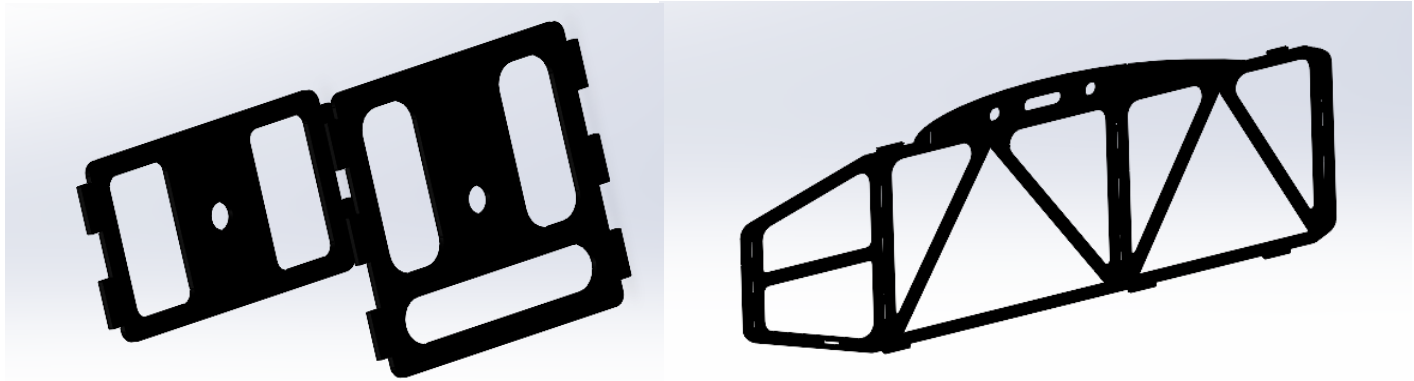


Figure 36- Fuselage Structural Components

3. A door stopper was also added to the internal structure to prevent the door from getting too backwards after dropping the payload.
4. In the front zone, a plywood floor was added and customized as needed to attach the battery and radio receiver onto it tightly without having to worry about them moving from their places during flight.

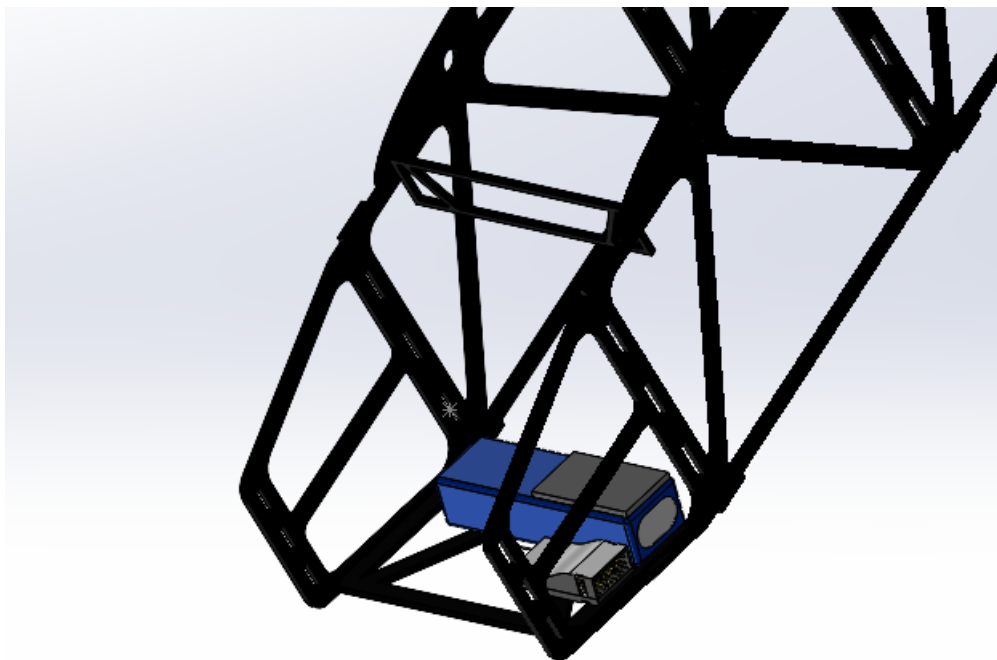


Figure 37- Stopper and Battery Floor Structure





5. Motor Mount

- A motor mount was used to connect the propulsion set to the fuselage and structure of the aircraft. It was designed to be easily mated with holes in the internal structure and on the skin.
- The motor mount was also designed to be strong enough to withstand the static thrust produced by the propulsion system.

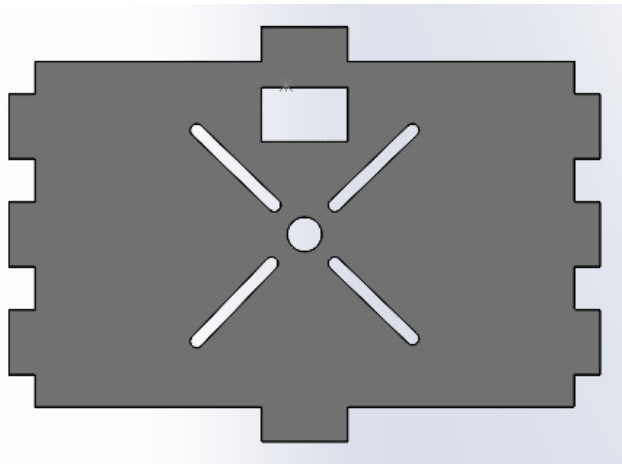


Figure 38-Motor Mount Structure

6. Medical Supplies Box (Payload)

- Our medical supplies box is made out of plywood and a hinge-lock pair was attached to it using bolts and nuts to lock the box and secure it properly.

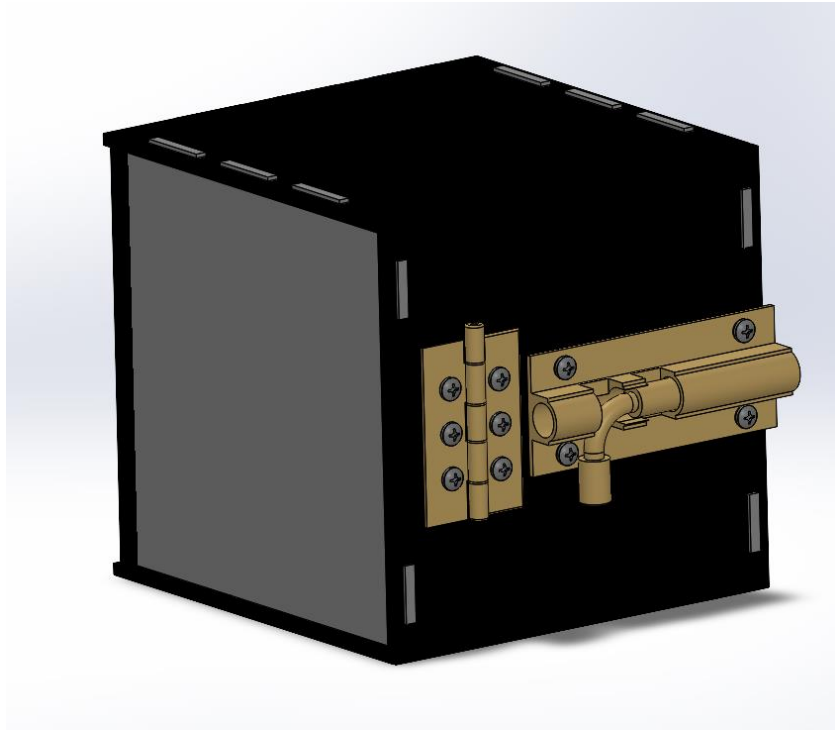


Figure 39- Supply Box Design





5.2.3 Wing and Spars

1. The wing was designed with a span of 1.587m, a chord of 0.25m, and an area of 0.403 m^2 with no taper ratio. The material used to manufacture the wing is blue foam. The airfoil used is SG6012.
2. The spars made for the wing are aluminium rods with a diameter of 1 centimetre and are 1.580 m long. The distance between the front and the rear spar is approximately 7.65 centimetres. The spars are used to connect both wings to the fuselage with a wing cap in the middle to protect the spars and increase their endurance during flight.
3. In addition, the ailerons of the wing were designed to have an area equal to 12% of the wing area. The wing connection also included winglets attached to the wing tips to support the aircraft's stability.

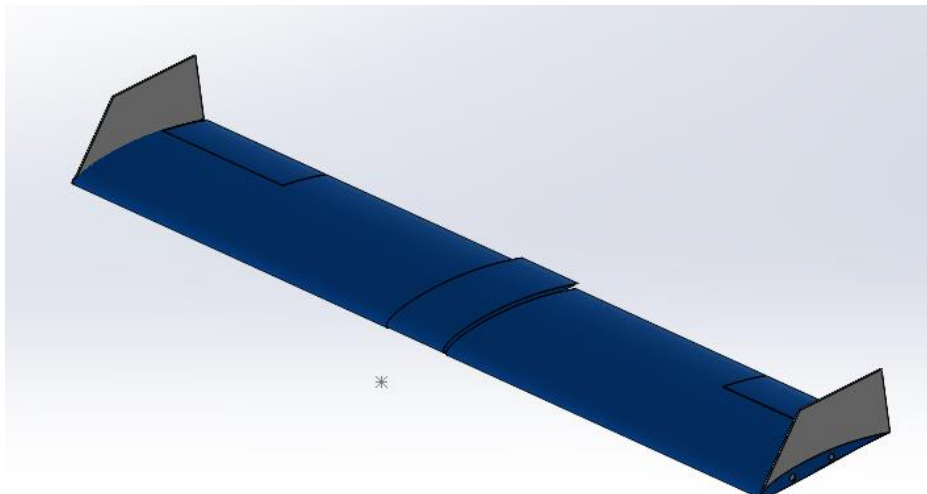
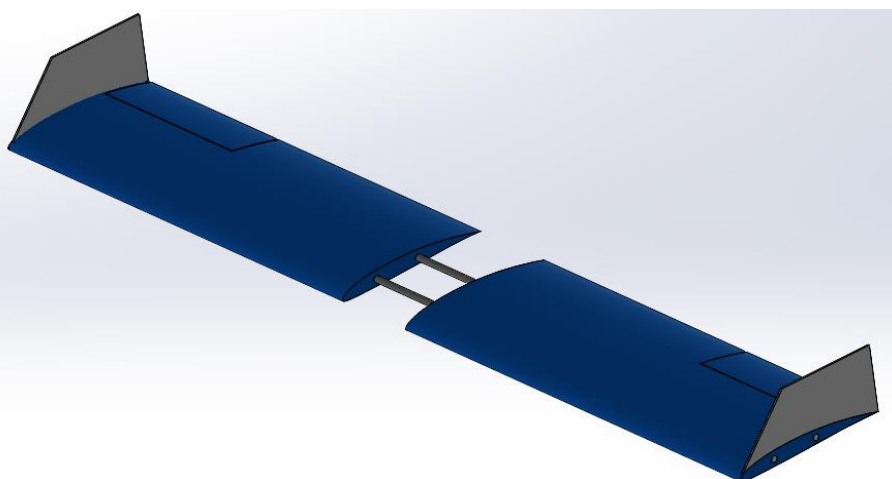


Figure 40- Wing and Spars Connection





5.2.4 Empennage and Tail Boom

1. The empennage was made as a flat plate with white foam; therefore, no airfoil was needed. The horizontal stabilizer is 44.6 cm long and the vertical stabilizer is 32.8 cm long. The horizontal stabilizer is tilted 2.5 degrees upward from the horizontal axis to keep UAV stability. The tail boom is 62cm long with 18cm of it getting inside the fuselage's bulkheads.

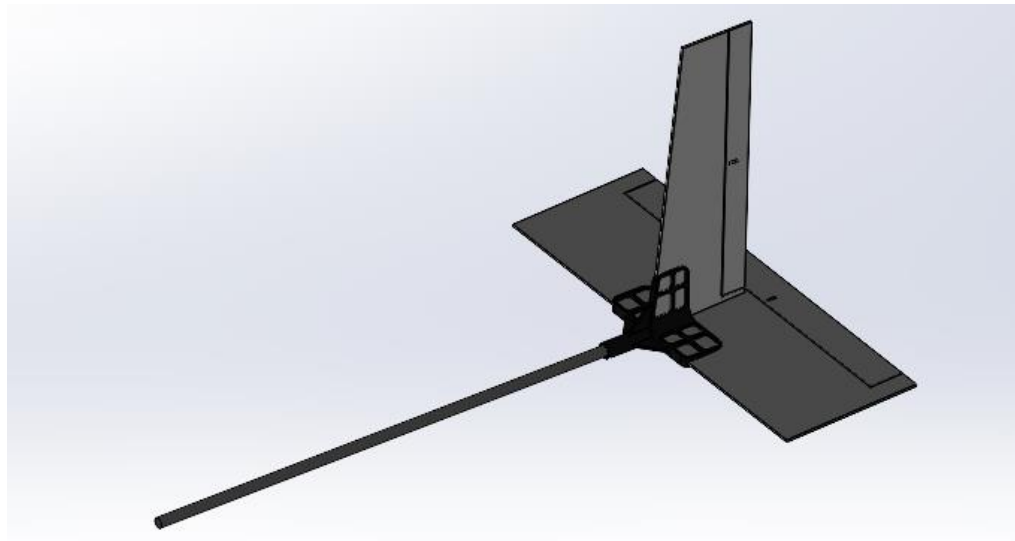


Figure 41- Empennage and Boom Connection

2. The tail connector is made out PLA material and was 3D printed. 3D printed parts can easily be redesigned using CAD software as necessary and therefore we were easily able to tilt the connector 2.5 degrees horizontally to shift the tail upwards by the same value. The tail connector is designed with rib patterns to stand against high loads and for any stresses to get distributed and not accumulate at any specific point near the connection points.



Figure 42- Tail Connector Design





5.2.5 Propulsion

From further performance analysis and tests, propeller APC-Slowfly SF was selected as the primary propeller for the final aircraft due to its sufficient thrust, enabling target flight speeds for all flight. On the other hand, the motor Turnigy, ESC, and battery LiPo 2200 of the propulsion system were unchanged from the preliminary design.

5.2.6 Avionics and Wiring

To obtain the least weight the avionics beside the wiring were very simple. There was no need for avionics battery to be on the aircraft only the main battery is enough to serve the spektrum 6 channel receiver to control 6 plastic geared servos of SG90 which are light compared to metal geared servos as MG90, the control surfaces and mechanisms.

5.3 Weight and Balance

The weight and balance of the *aircraft* was analysed by using measured weights of propulsion and avionics components. The location of these components is determined according to balance the aircraft around the CG point which had been determined from XFLR5 to be at 8.6 cm from the leading edge of the wing. We have determined the position of each propulsion and avionic component taking our reference point the top right corner of the motor mount.

Component	X displacement (mm)	Y displacement (mm)	Z displacement (mm)
Propeller	-56.1	-62.5	-40
Motor	-25	-62.5	-40
Receiver	43.3	-23.3	-83.2
ESC	80.7	-27	-73.6
Battery	76.8	-52.5	-86.5
Right aileron servo	245.2	703.7	24.5
Left aileron servo	245.2	703.7	24.5
Elevator servo	993.5	-31.7	-28.7
Rudder servo	980.9	-54.5	122.2

Table 19- Balancing Components Displacements

5.4 Material Quantity

The following tables shows the materials, the quantity and our buy list.

5.4.1 Internal Structure

Part Name	Part Height	Part Width	Part Depth	Material	No of Parts
Side	176	480.5	3	Plywood	2
Motor Mount	106	147	3	Plywood	1
Front	130	147	3	Plywood	1
Door Stopper	40	141	3	Plywood	1
Intermediate	130	147	3	Plywood	1
Rear	86	147	3	Plywood	1





Battery Floor	90	147	3	Plywood	1
Box	130	130	3	Plywood	6

Table 20- Structure Area, material and number of parts

Area Required for Part (mm ²)	Material Standard Area	Quantity Required		
84568				
15582				
19110				
5640			PLYWOOD	For Internal Structure and The Box of The Payload
19110	2250000	1		
12642				
13230				
16900				
186782				

Table 21- Structure Buy List

5.4.2 Rods

Part Name	Length	Outer Diameter (mm)	Inner Diameter (mm)	Material	Number of parts
Boom	630	12	11	Aluminum	1
Front Spar	1591	10	9	Aluminum	1
Rear Spar	1591	10	9	Aluminum	1

Table 22- Rods area, material and number of parts

Length Required	Material Standard Length (mm)	Quantity Required		
630		4000 For Spars	Aluminum	For Spars and Boom
1591				
1591	By Order	650 For Boom		
3812				

Table 23- Rods Buy List





5.4.3 Wing

Part Name	Length (mm)	Thickness (mm)	Chord Length (mm)	part Material	Number of Parts
main wing	722	26.3	254	Blue Foam	2
Cap Wing	125	26.3	265	Blue Foam	1
Winglet	116	264	3	white Foam	2

Table 24- Wing area, material and number of parts

Area Required	Standard Area	Quantity Required		
183388				
183388			BLUE FOAM	Wing and Wing Cap
33125		1		
399901	915000			

Table 25- Wing Buy List

5.4.4 Tail and Skin

Part Name	Length (mm)	Thickness (mm)	Chord Length (mm)	part Material	Number of Parts
Vertical Stabilizer	198	3	124	white Foam	1
Horizontal Stabilizer	508	3	176	white Foam	1
Skin	630	3	606	white Foam	1

Table 26- Tail and Skin area, material and number of parts

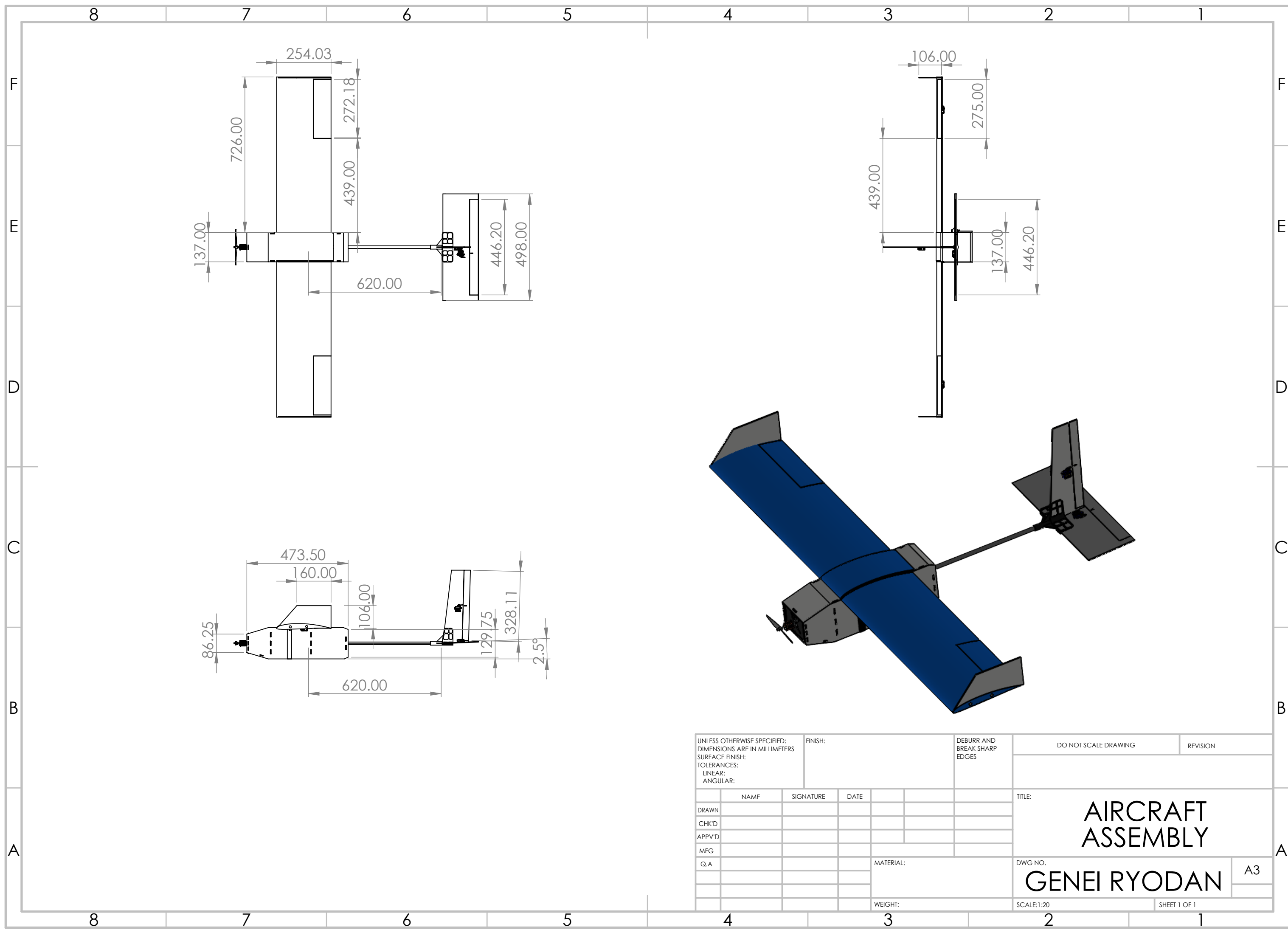
Area Required	Material Standard Length (mm)	Quantity Required		
24552				
89400			WHITE FOAM	For Tail, Skin and Winglets
30624	700000	1		
144576				

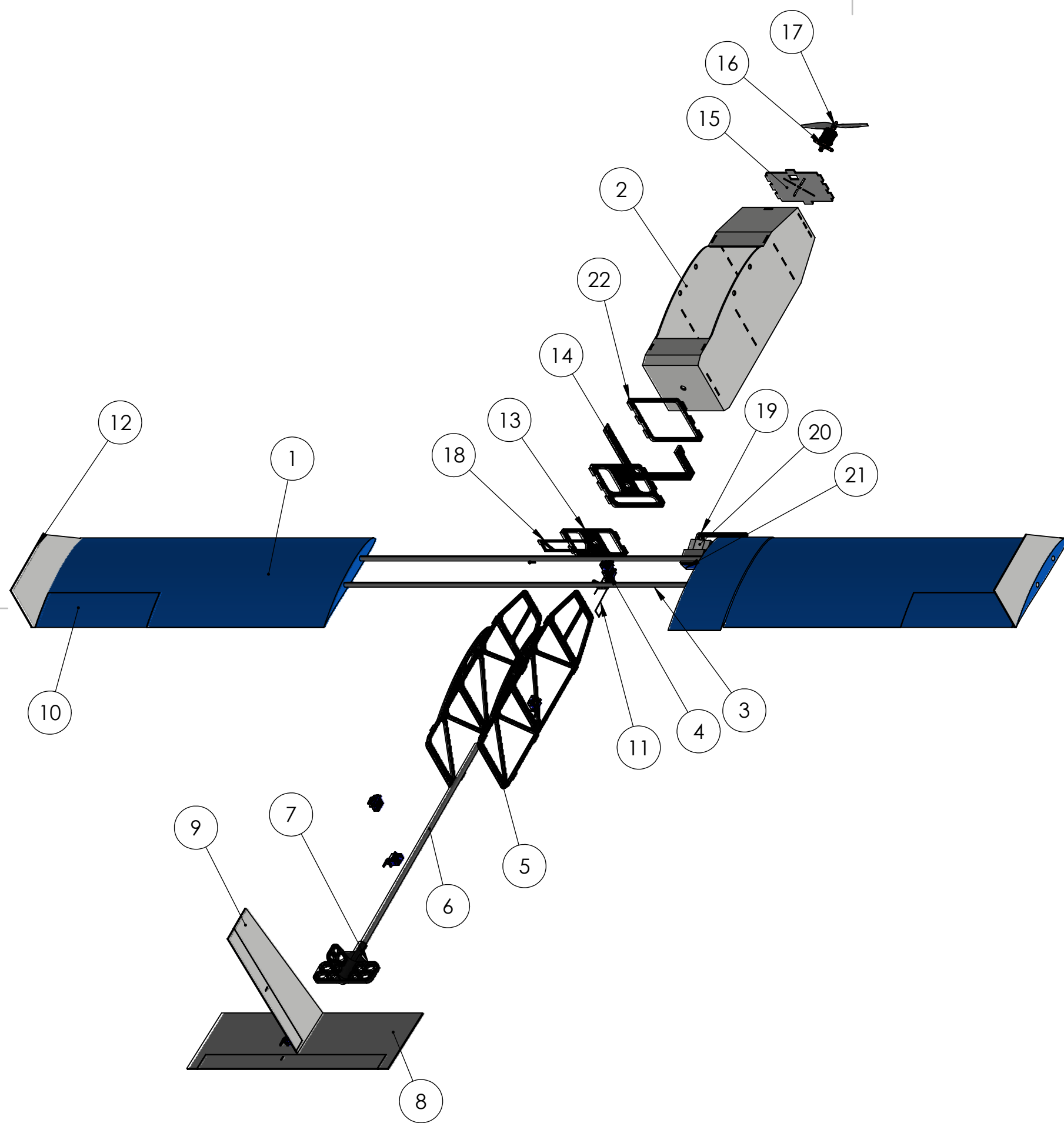
Table 27- Tail Buy List

5.4 Drawings

The drawing package contains a dimensioned 3-view of the aircraft, exploded views of the primary structure of the aircraft, locations of the electronics within the aircraft, and detailed views of the subsystems of the aircraft.







ITEM NO.	COMPONENT	DESCRIPTION	QUANTITY
1	WING	BLUE FOAM	2
2	FUSELAGE	WHITE FOAM	1
3	SPAR	ALUMINUM	2
4	ONE-ARM SERVO	SERVO SG90	6
5	INTERNAL STRUCTURE	PLYWOOD	2
6	TAIL BOOM	ALUMINUM	1
7	TAIL CONNECTOR	FIBER COMPOSITE	1
8	HORIZONTAL STABILIZER	WHITE FOAM	1
9	VERTICAL STABILIZER	WHITE FOAM	1
10	AELIRON	BLUE FOAM	2
11	IRON ARM	STEEL	2
12	WINGLET	WHITE FOAM	2
13	REAR BULKHEAD	PLYWOOD	2
14	RUBBER BAND	RUBBER	1
15	MOTOR MOUNT	PLYWOOD	1
16	MOTOR	TURNIGY 035484(1100)	1
17	PROPELLER	APC SLOWFLY 10IN.	1
18	DOOR STOPPER	PLYWOOD	1
19	FLOOR	PLYWOOD	1
20	RADIO RECEIVER	V8FRII-RECEIVER	1
21	BATTERY	LiPo 2200mAh 25/35C	1
22	FRONT BULKHEAD	PLYWOOD	1

TITLE: EXPLODED UAV
VIEW
DWG NO. GENEI RYODAN A3
SCALE:1:10 SHEET 1 OF 1

8 7 6 5 4 3 2 1

F

F

E

E

D

D

C

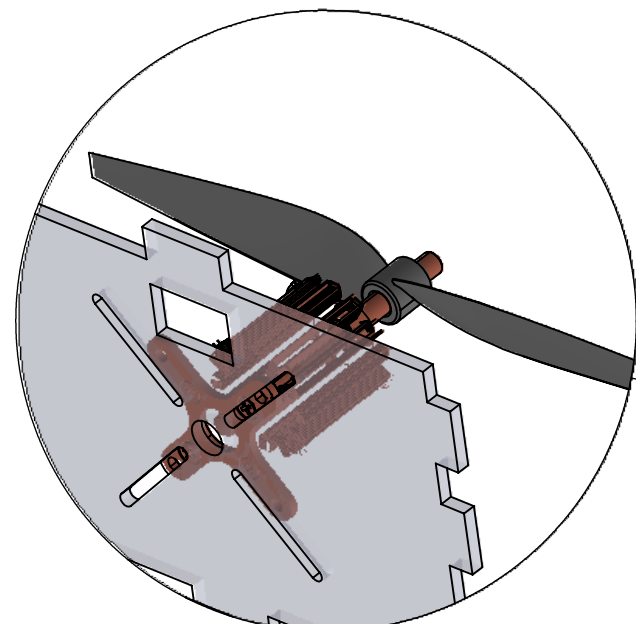
C

B

B

A

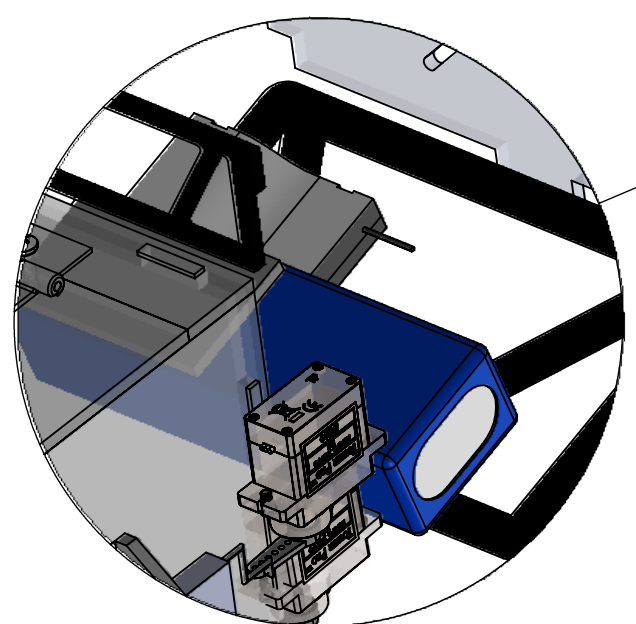
A



DETAIL A

SCALE 1 : 1.5

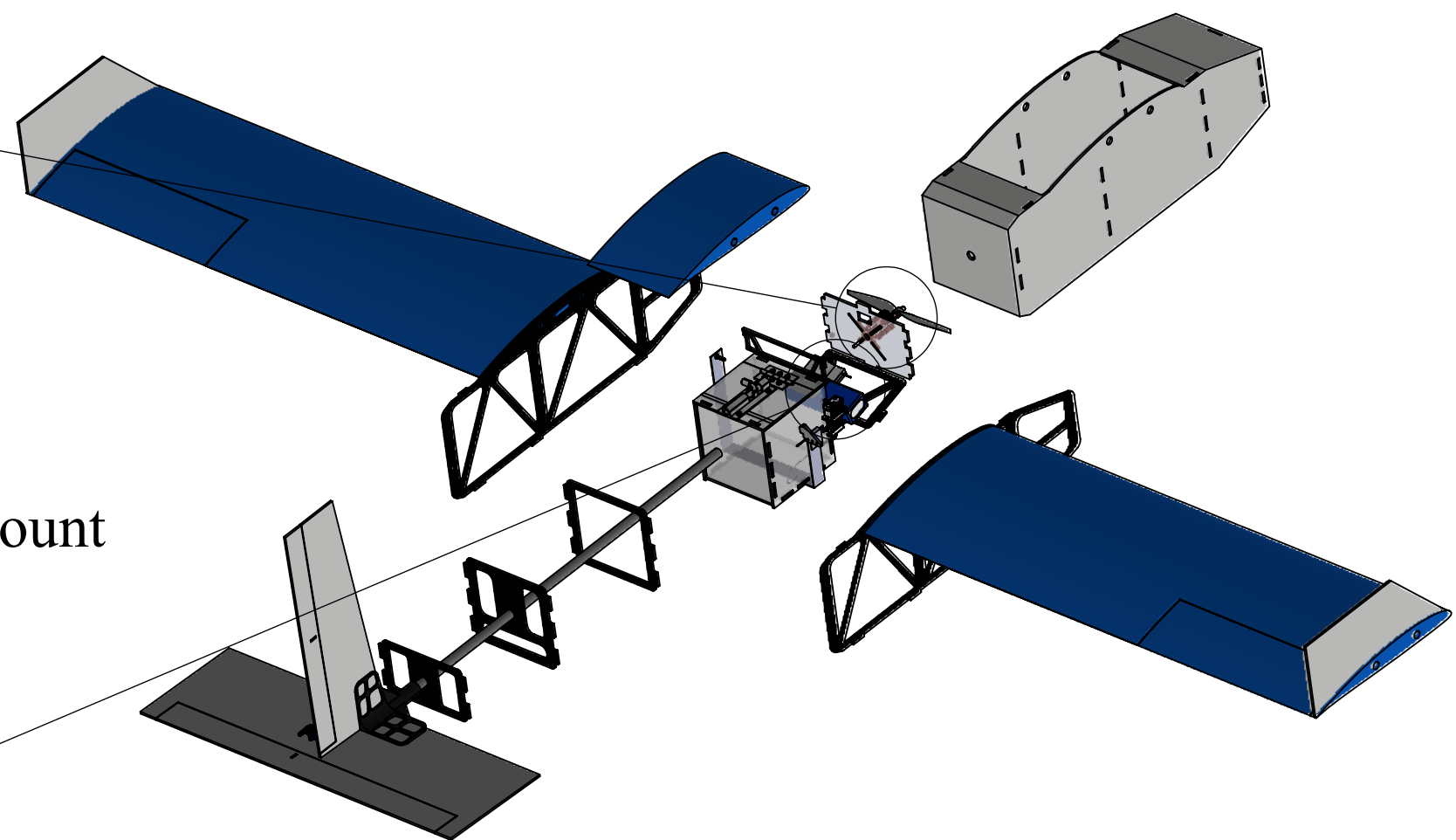
Propulsion Set attached to Motor Mount



DETAIL B

SCALE 1 : 1.5

Battery and Receiver tightened
on Wooden Floor



TITLE:
**UAV EXPLODED
VIEW 2**
TEAM:
GENEI RYODAN A3
SCALE:1:10
SHEET 1 OF 1

8 7 6 5 4 3 2 1

8 7 6 5 4 3 2 1

F

E

D

C

B

A

F

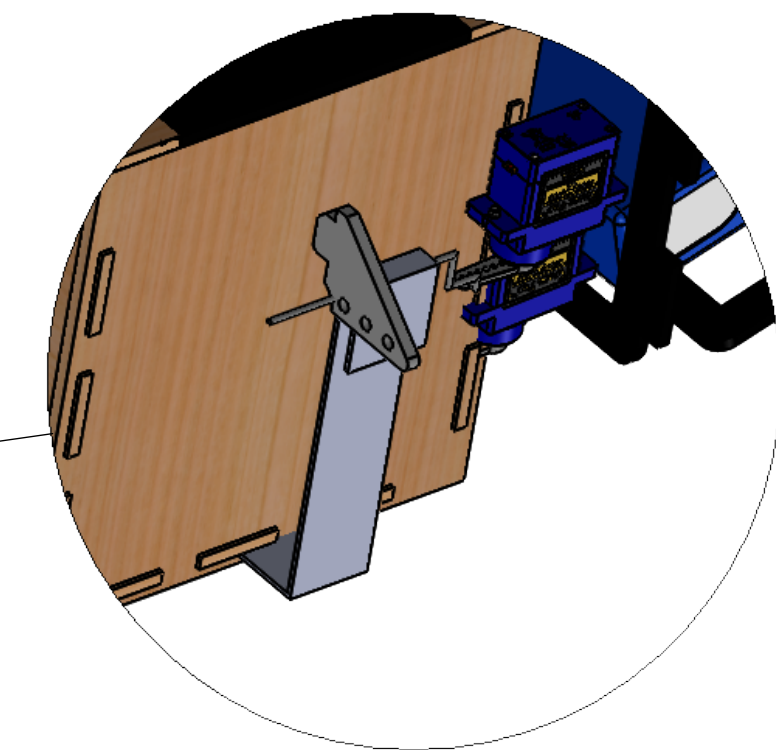
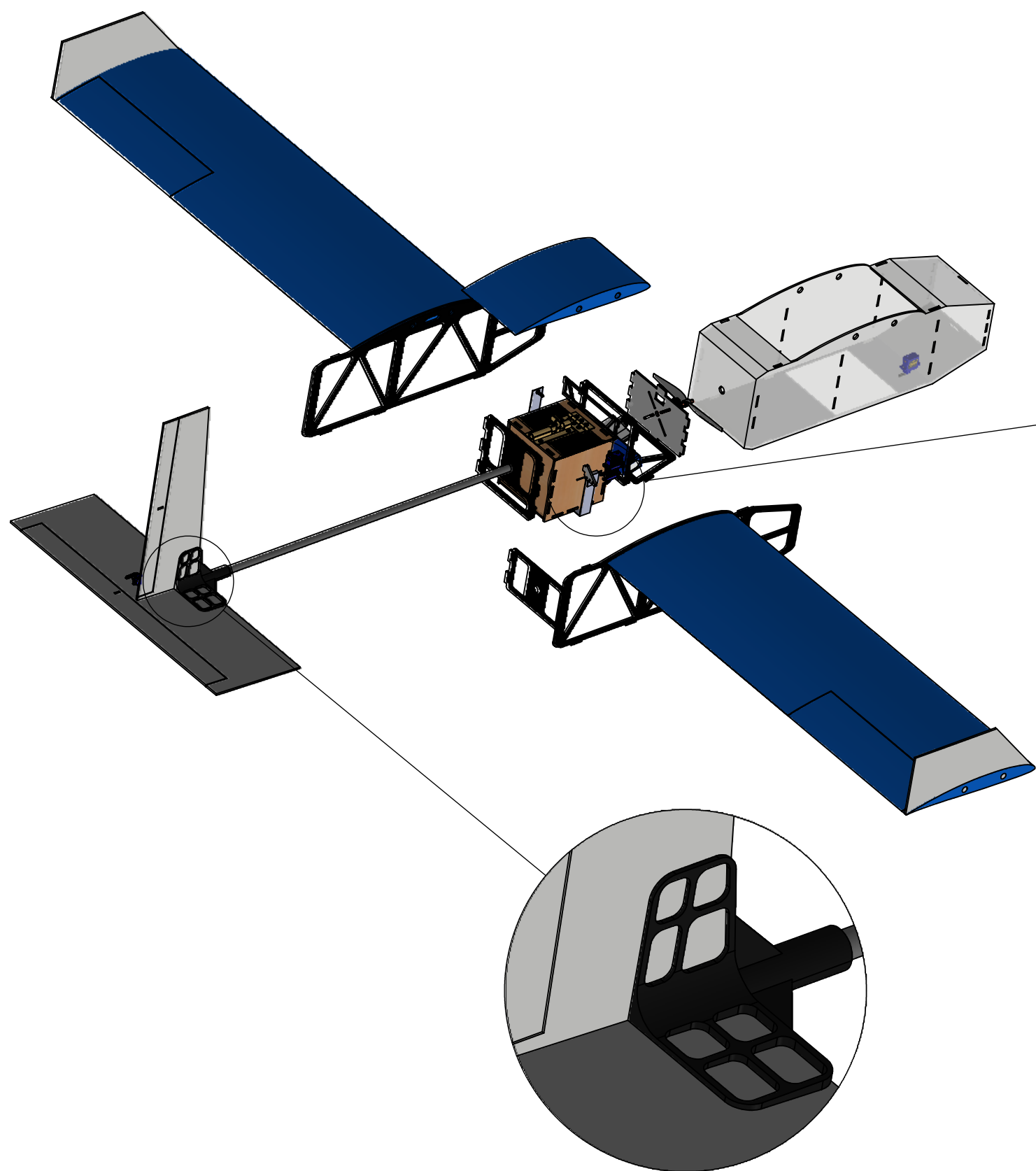
E

D

C

B

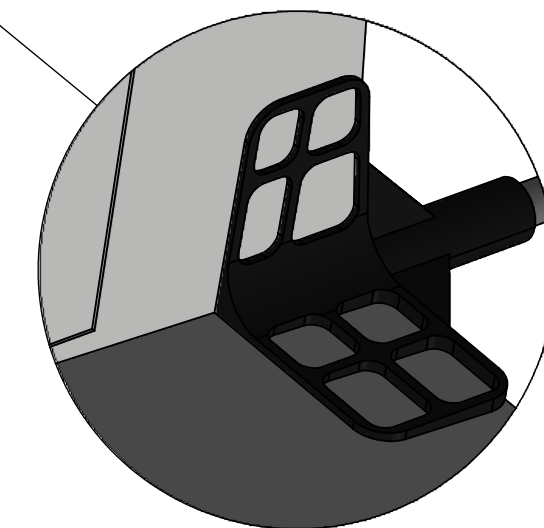
A



DETAIL A

SCALE 1 : 1.5

Rubber band and Servo Mechanism
to Drop the Payload



DETAIL B

SCALE 1:2

3D Printed Ribbed Tail Connector

TITLE: UAV EXPLODED VIEW
WITH PAYLOAD
TEAM: GENEI RYODAN
A3
SCALE:1:10
SHEET 1 OF 1

8 7 6 5 4 3 2 1



6.0 Manufacturing Plan

In this section, we will provide an overview of the manufacturing processes and assembly stages employed in the construction of this UAV.

6.1 Manufacturing Processes Description

6.1.1 Hot Wire Cutting

Hot wire cutting foam is a precise and efficient technique used in manufacturing and crafting to cut foam materials. This method involves using a heated wire, typically made of nichrome or other heat-resistant materials, to cleanly slice through foam sheets or blocks. The wire's high temperature allows it to melt through the foam, creating smooth and accurate cuts, which are especially beneficial for creating custom shapes, in our case, cut the foam into an airfoil shape.



Figure 43- Hot Wire Cutting The Wing

As shown in Figure 1 after uploading the .dxf file to the profili program which generates gcode and sends the code to the Hot Wire Cutting machine controller (mach3) with the Coordinates and starts cutting the blue foam sheet to the desired airfoil shape.

6.1.2 Laser Cutting

Laser cutting is a highly precise and versatile technology used to precisely cut various materials. It involves the use of a focused laser beam to vaporize or melt the material, creating a clean and accurate cut. This process is widely used in industrial, manufacturing, and even hobbyist applications for cutting materials such as metals, plastics, wood, textiles, and more. Furthermore, laser cutting has been determined to be the fastest method for manufacturing 2D plywood parts, with simple parts being cut in under 5 minutes.



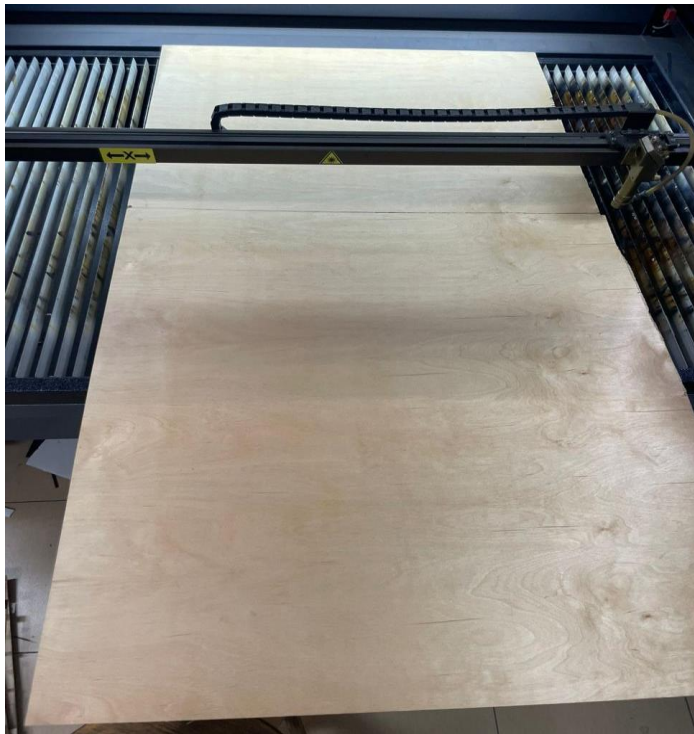


Figure 44- Plywood Sheet Before Laser Cut Starting

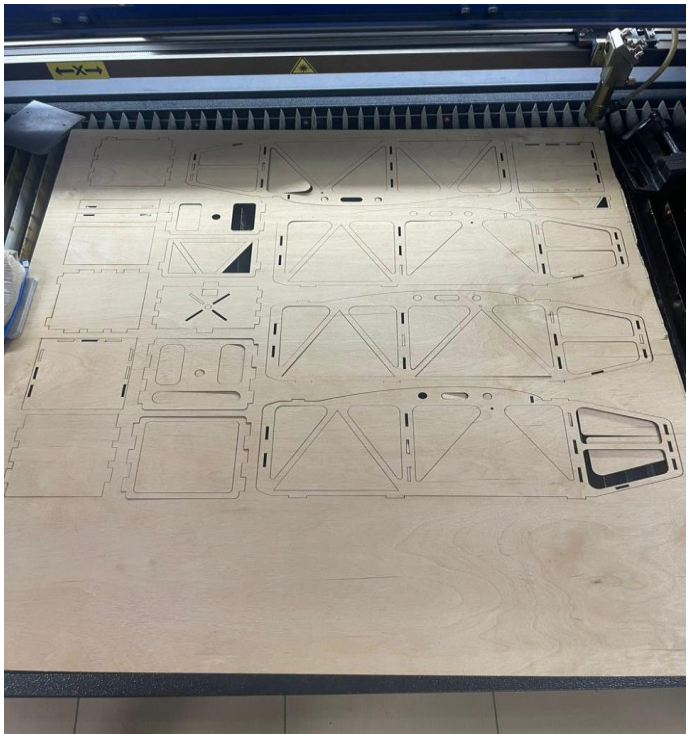


Figure 45-Plywood Sheet After Laser Cutting

Furthermore, we utilized laser cutting to fabricate the skin of the UAV. This skin is crafted from white foam. After flattening the skin within the CAD program, we uploaded the drawing to the CNC system, which controls the laser cutter.

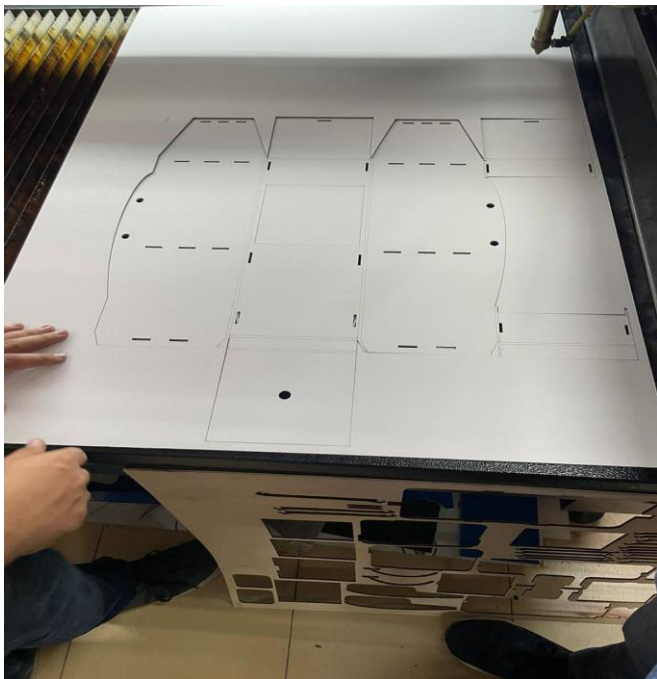
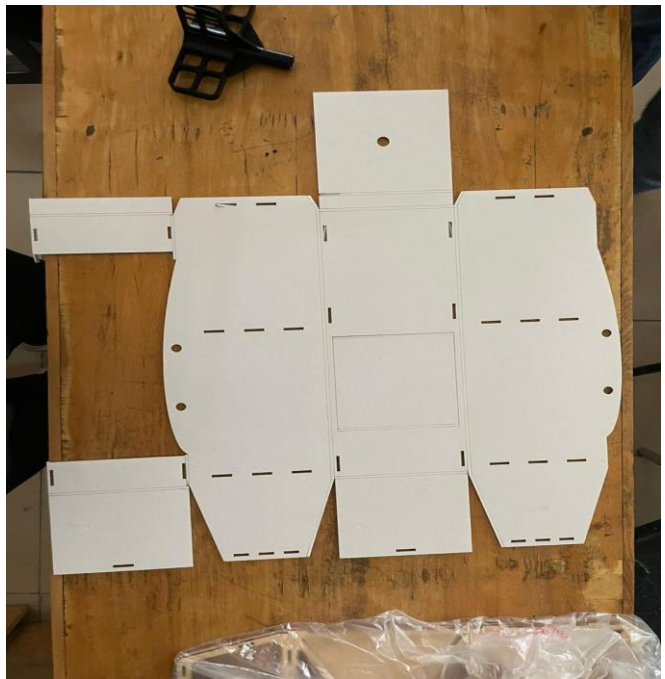


Figure 46- Skin After Laser Cutting





6.1.3 3D Printing

This innovative process allows for the creation of three-dimensional objects by adding material layer by layer, as opposed to traditional subtractive methods that involve cutting away from a solid block of material.

Using 3D Printing, We Created a Tail Connector from Polylactic Acid (PLA) instead of making one from plywood to reduce weight and increase Stiffness.



Figure 47- Tail Connector After Manufacturing

6.2 Manufacturing Overview

6.2.1 Fuselage

The fuselage serves as a critical component in an aircraft's structure, acting as its main body or central framework. In a particular project involving the assembly of a fuselage, our focus was on housing a medical supply box within this design. To begin the assembly process, we laser-cut the fuselage parts from plywood. Our assembly approach involved employing secure fixing methods to ensure robust connections between the various fuselage components. Initially, we aligned the component teeth with corresponding holes, and subsequently, we used super glue to firmly attach the bulkhead, motor mount, and tail mount to the sides of the fuselage.

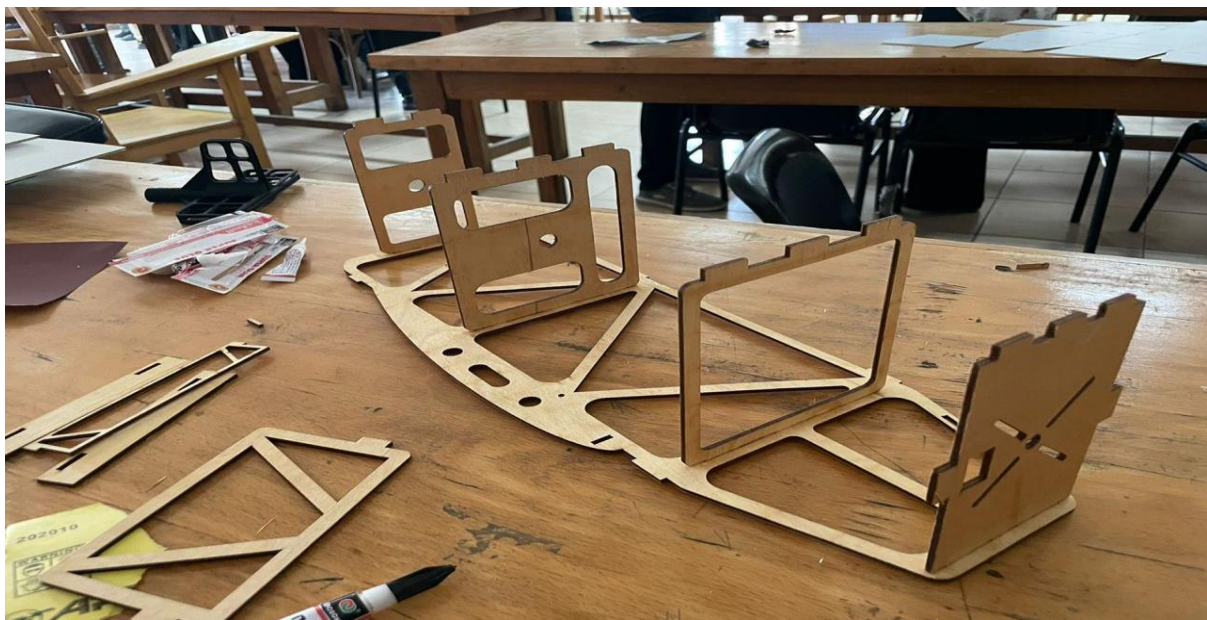


Figure 48- Fuselage Assembly





6.2.2 Wings

Wings serve as fundamental components in most fixed-wing aircraft, including airplanes and gliders. They play a critical role in generating lift and facilitating aircraft control during flight. In the construction process of these wings, we initiated the production by employing hot wire cutting techniques using Turkish Blue Foam. The primary wing structure is divided into three main sections: the left wing, right-wing, and cap wing.

After cutting the main sections of the wings, the subsequent step involved using a hot wire to cut flap sections in both the left and right wings. Following this, we proceeded to cut the wing spars to a specific length of 1581 mm to ensure they fit precisely within the wing assembly.



Figure 49- Wing and Airfoil



Figure 51- Ailerons Cutting



Figure 50- Spars and Boom Cutting





6.2.3 Empennage

The empennage, also known as the tail assembly, comprises both vertical and horizontal stabilizers in our design. We opted for a flat plate design for both stabilizers, constructed using 3 mm thick white foam material. The construction process involved cutting the white foam into the desired plate shapes and 3D printing the tail connector part. Next, we attached both the vertical and horizontal stabilizers to the tail connector, ensuring their proper alignment. Subsequently, we affixed a boom to the fuselage section (Tail mount), connecting it to the tail connector, and secured this attachment using epoxy adhesive.

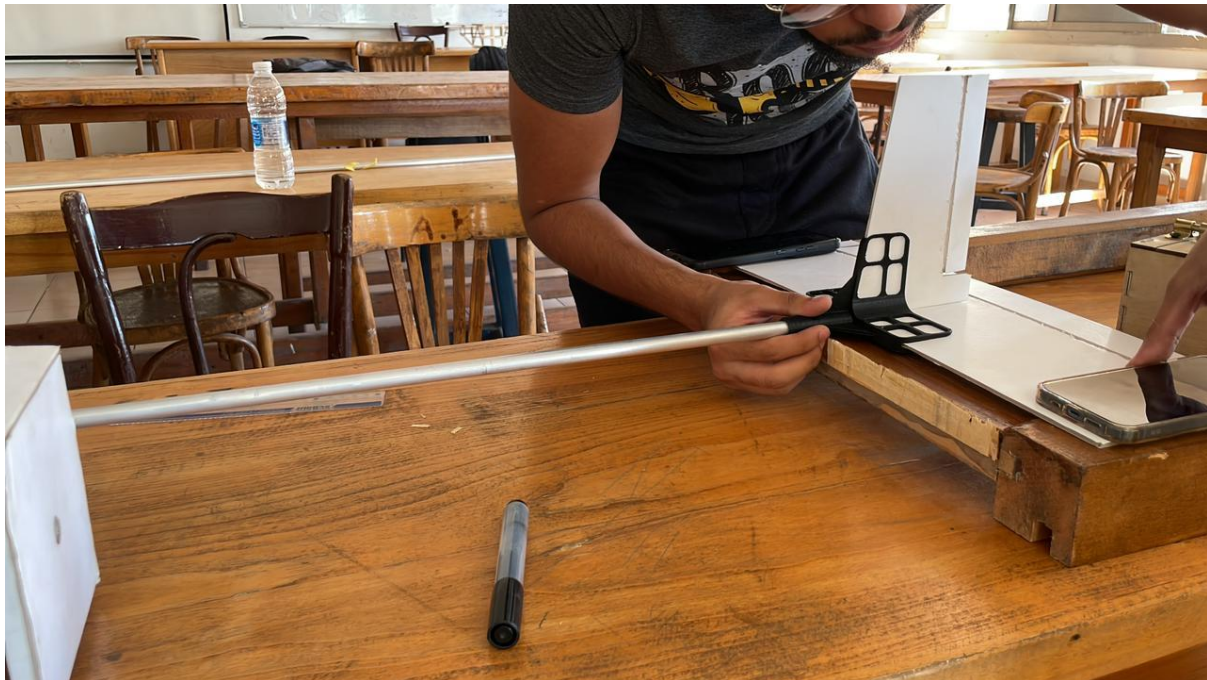


Figure 52-Tail Assembly

6.2.4 Electrical Components

In the context of UAVs (Unmanned Aerial Vehicles) and other aircraft, servos are often used to control movable components in our case ailerons, elevators, rudders, and supply box door. By receiving electrical signals from a flight controller or a pilot's input, servos can precisely adjust the position of these components, influencing the aircraft's orientation and flight characteristics. After securely mounting the servos, our next step was to create the electrical connections. We attached two servos to both sides of the wing, utilizing a delta configuration to ensure synchronized operation. Following that, we affixed two servos to the tail assembly, responsible for controlling and fine-tuning the rudder and elevator. Lastly, we connected these servos to the receiver using wiring and finally connected the receiver to the battery.



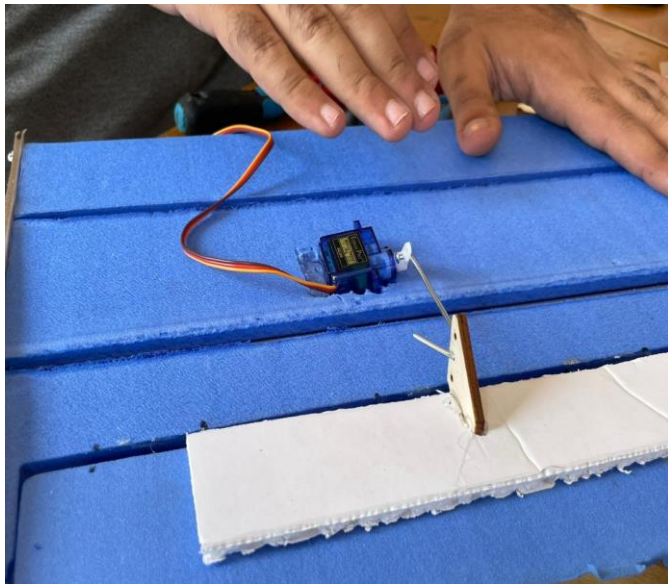


Figure 54- Aileron's Servo Mounting

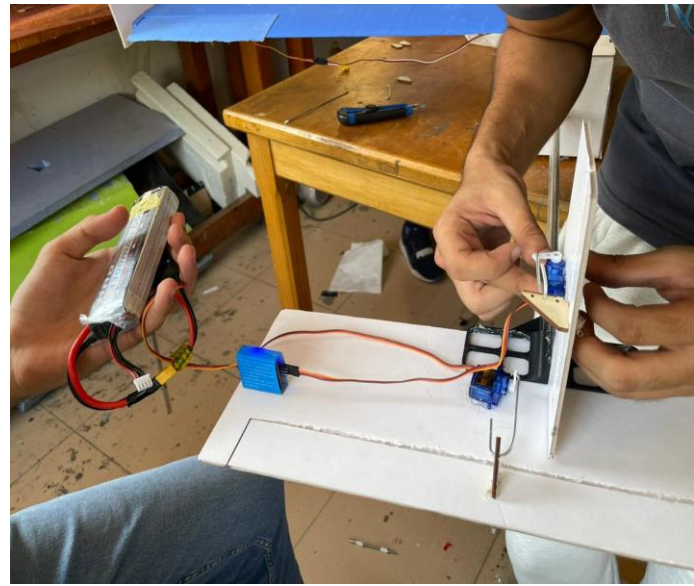


Figure 53- Tail's Servos Mounting

6.2.5 Skin and Supply Box

The last step in our process involved affixing the skin onto both the fuselage and the supply box. The skin material, consisting of 3mm thick white foam, was used for this purpose. Initially, we flattened the design of the skin in SolidWorks, and then we transferred the file to the RD Works program, which controlled the laser cutter. Once the cutting was completed, we commenced the process of attaching this flattened sheet to the UAV, firmly securing it in place using adhesive.



Figure 56- Flattened Skin Before Assembly



Figure 55- Skin After Assembly





Once the UAV manufacturing process was completed, the next step involved constructing the Supply Box, which serves as the payload compartment for the UAV. This Supply Box measures (12x12x12 cm) and is crafted from plywood. To begin, we cut the plywood into sheets and then assembled them, like the method used for the UAV's fuselage, using interlocking teeth and holes. We secured the box's edges by applying adhesive, ensuring a sturdy connection.

Subsequently, we proceeded to attach a door and a locking mechanism consisting of a door lock and hinge to facilitate the opening and secure closure of the box. This was essential to guarantee that the payload inside the box remained securely contained during flight. Ultimately, we crafted a parachute using Celia fabric and securely fastened it to the upper edge of the supply box. To enhance payload and drop safety, we integrated a 25G shock sensor, ensuring the parachute deploys automatically upon release.



Figure 57-Manufactured Parachute



Figure 58- Manufacture Box

7.0 Testing

Within this section, we will present a comprehensive overview of the testing procedures and various test categories utilized following the construction of a UAV. These tests are instrumental in verifying the UAV's compliance with specific mission requirements.

7.1 Structural Test

UAV structural testing plays a pivotal role in the development and assessment of Unmanned Aerial Vehicles (UAVs). This process entails subjecting the physical framework and components of the UAV to meticulous assessments aimed at ensuring their integrity and reliability. These examinations encompass





a variety of evaluations, such as stress testing, load testing, vibration testing, and more, all devised to replicate real-world conditions and forces that a UAV may encounter during its missions. The primary objective is to pinpoint any weaknesses or vulnerabilities in the UAV's structure and rectify them to enhance safety and performance. The successful execution of UAV structural testing is imperative in ensuring that the aircraft can withstand the demands of its designated missions and operate effectively across diverse environments. For example, we conducted a Motor Mount Test on our UAV fuselage to assess its ability to withstand the designed static thrust of the motor. This test comprises using a sandbag with a weight equivalent to or greater than the thrust generated by our motor (our Motor Static Thrust 2074g), which is then affixed to the motor mount section in the fuselage as in Figure 2. Subsequently, we suspend the fuselage and assess its capability to bear the weight



Figure 60- Motor Mount Test Weight



Figure 59- Succession of Motor Mount Test

After completing the Motor Mount Test, the next steps involved conducting the Boom Deflection Test and assessing the horizontal Stabilizer's stability. Following the assembly of the UAV, we performed calculations in the Trim Flight scenario, determining that the weight would equal the lift using the formula: $L = \frac{1}{2} \rho v^2 C_L S$, where v represents the cruise velocity, S signifies the tail wing area, and C_L assumed to be 1.3 for a flat plate airfoil. The result





indicated that the weight equated to 10 N, which is equivalent to a mass of approximately 1 kg. We proceeded to test loads of 1 kg and 1.5 kg on the boom and observed no deflection in the case of a 1 kg load, but a slight deflection when applying a 1.5 kg load.



Figure 61- Succession of Boom Deflection Test

7.2 Mechanisms and servos Test

We can divide our mechanism in to two sections.

1. Box dropping mechanism

This mechanism is very simple as it consists of clothes rubber band which is elastic and at the same time is thick so it can hold the box safely preventing the box from dropping from the aircraft, this rubber band is fixed on the right fuselage by screw then it passes below the aircraft to hold the box and fixed from the other side on the arm of the servo.

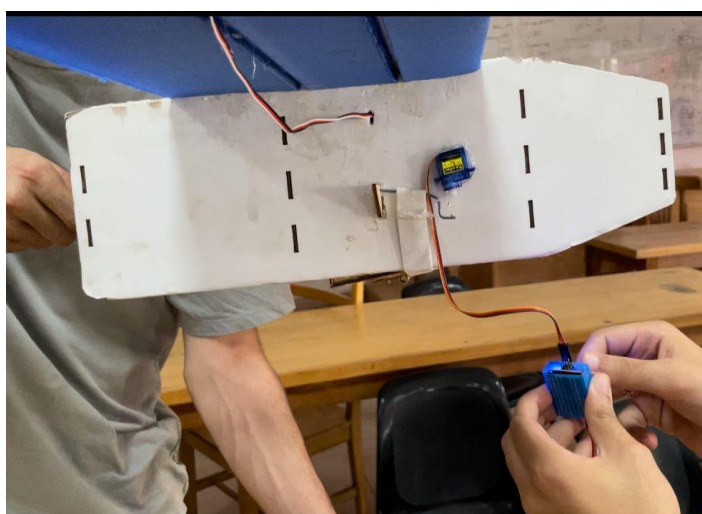


Figure 63- Payload Box before being dropped

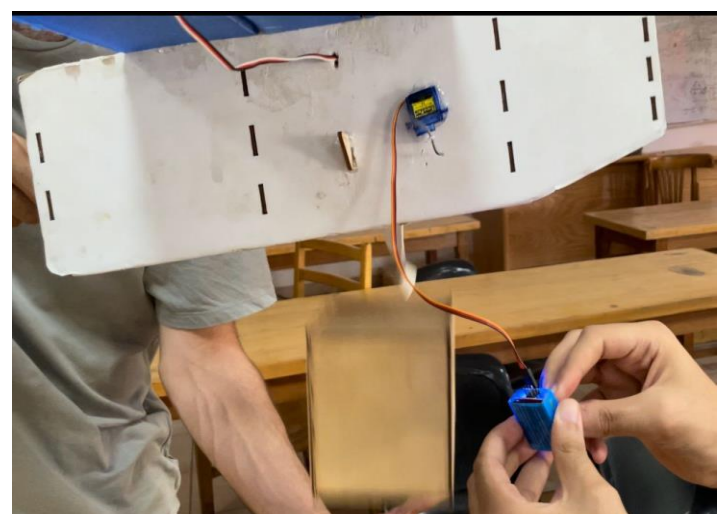


Figure 62- Payload Box after being dropped





The payload (box and parachute) works as the door of the airplane right now which means that they both leave no area for air to sneak to the fuselage and the actual door is opened by 90 degrees, also there is a stopper that make sure that the door will not open more than 90 degrees to leave no area for air. Simply by giving the signal to servo to rotate the arm will leave the horn and the band's resistance to tension will make it dissociate itself from the arm.

2. Door mechanism

This mechanism is also very simple because as we had illustrated that the payload will work as the door of the aircraft, but after dropping the payload it will leave behind its huge area for air to sneak so this is the time for door mechanism to play its rule. As mentioned, the door is opened by 90 degrees and there is a stopper for the door to prevent it from opening more than 90 degrees, another servo existing for close that door fix it in its place by its arm to leave no area for air to sneak through the door.



Figure 65- Door Opening

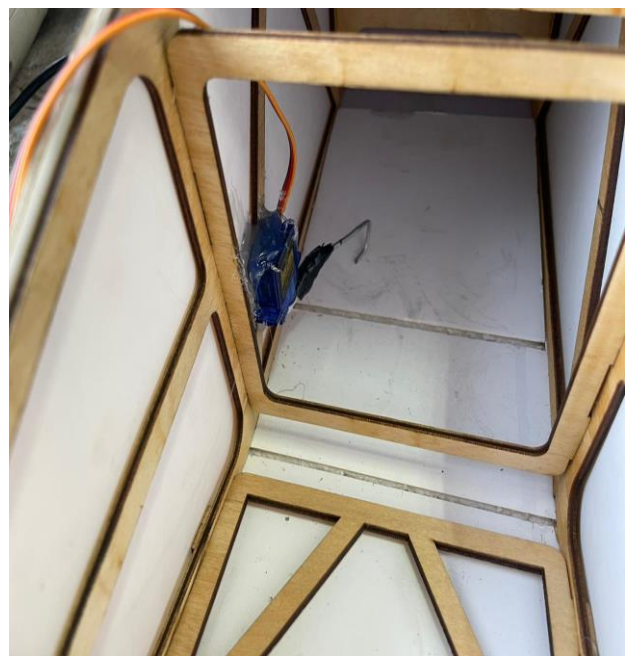


Figure 64- Door Closing

The flight mechanisms test is a pivotal phase in the evaluation of Unmanned Aerial Vehicles (UAVs) designed to ensure their aerodynamic and flight-related systems are in optimal working condition. During this rigorous examination, various aspects of the UAV's flight mechanics are thoroughly assessed. This includes scrutinizing elements like propulsion systems, control surfaces,





stability, maneuverability, and overall flight performance. Engineers and operators conduct a series of flight maneuvers and simulations to validate that the UAV can achieve the desired flight characteristics, respond effectively to control inputs, and navigate safely through different operational scenarios. The data collected from these tests not only guarantees the UAV's capability to execute its mission tasks but also informs adjustments or enhancements in the flight mechanisms, ultimately ensuring reliable and efficient UAV operations.

7.3 Parachute Test

The payload parachute test is a critical phase in the evaluation of Unmanned Aerial Vehicles (UAVs) and their ability to safely deliver payloads. During this test, the functionality and reliability of the parachute system designed to deploy and control the descent of payloads are rigorously assessed. The payload parachute test is essential in verifying that the UAV can successfully transport and release its cargo while maintaining the safety and integrity of the payload. Upon completing the sewing of the parachute, the team affixed it to the box and proceeded with a test. The initial test was carried out in the Aerospace Engineering Building, excluding the 25G shock sensor. The objective of this test was to assess the parachute's ability to decelerate the payload effectively during the descent, ensuring a safe landing.



Figure 66- Succession of Parachute Test

7.4 Flight Test

The UAV flight test phase represents a pivotal milestone in the development and validation of Unmanned Aerial Vehicles (UAVs). During this crucial stage, the UAV is taken to the skies to evaluate its performance, capabilities, and overall functionality in a real-world setting. Flight tests encompass a wide range of assessments, including stability and control checks, navigation and communication system validations, payload performance evaluations, and endurance trials. These tests aim to verify that the UAV can successfully carry out its intended missions. The data collected from these flight tests not only





validate the UAV's design but also inform any necessary refinements or improvements, ultimately ensuring that the UAV operates reliably and effectively in its designated operational environments.

7.4.1 First Flight Test

The first flight test occurred on Thursday, September 21st, and it was conducted without the payload onboard. Prior to the flight, the UAV underwent a comprehensive pre-flight inspection, which involved attaching its RC control unit (receiver) and verifying its takeoff weight, recorded at 0.94 kg before propulsion insulation and 1.58 kg after propulsion installation. The first flight test was a resounding success for our UAV; the takeoff was seamless, and the aircraft demonstrated excellent stability and control throughout the flight. The UAV completed three turns around the stadium track before executing a smooth landing. The feedback garnered from this initial flight test highlighted the UAV's exceptional airborne stability without the payload. Consequently, we plan to proceed with a second flight test to conclude the testing of the payload release mechanisms and parachute deployment, incorporating the 25G shock sensor for further evaluation.



Figure 67- Aircraft weight before Propulsion installation

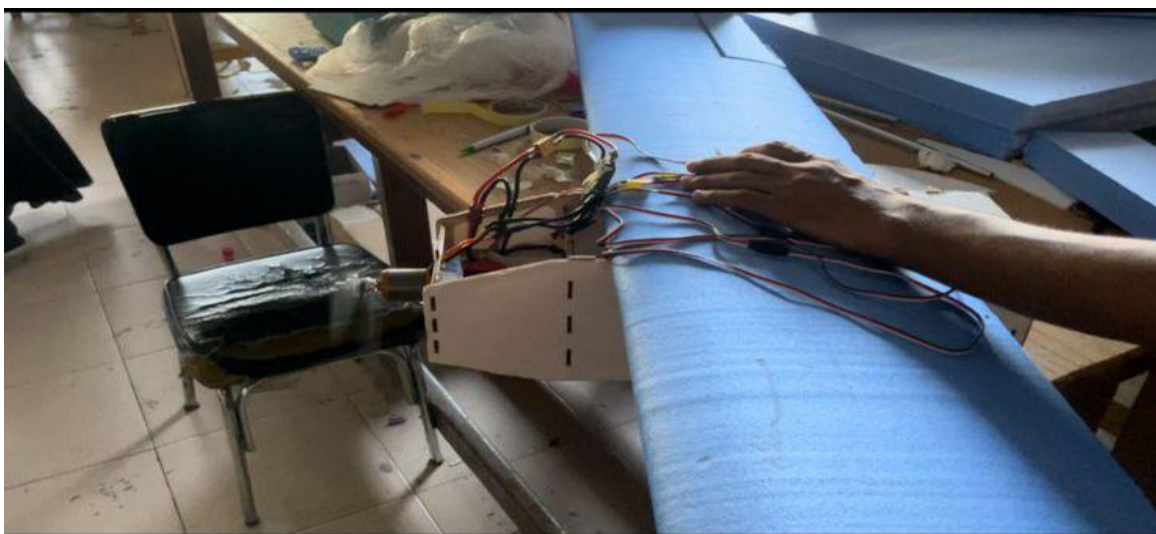


Figure 68- Avionics Testing





Figure 69- Hand Launched Aircraft



Figure 70- Takeoff Succession





Figure 71- High Maneuverability performance



Figure 72- Landing Succession





8.0 Future Work

Finally, there is nothing will be completely perfect as there will always be some obstacles in the journey but the real gain represented in the good mentors who made us have fun and helped us to gain information, techniques and tools that really improved our knowledge, these obstacles represented in the subsystem of the aircraft that we have noticed through the journey and improving these flaws will lead to better performance and more functionality.

8.1 Aerodynamics

- Increasing the stability of phugoid mode as the conjugate poles are really so close to the imaginary.
- Dihedral wings to give more stability to the aircraft instead of increasing the displacement of the wings in the z axis which means increasing the weight of the structure.

8.2 Propulsion

- Doing more research outside the box to optimize the performance of the propulsion and its weight.

8.3 Structure

- Doing stress analysis on the fuselage may lead to decreasing the size of the truss which will lead to more optimization in the weight.
- Stress analysis on the boom to optimize the best points of fixation to increase its life time and give the boom more rigidness in case of unnormal flight.
- More aerodynamically structure for more smooth passing of the air on the skin specifically the aft part of the fuselage which has very short taper.
- Manufacturing of small hinge and lock-pin for the payload box will lead to decrease in its weight which means more weight for medical supplies.
- Increase the length of nose area to leave more distance to the propulsion components to put the CG in its desired point.

8.4 Manufacturing

- More space for accessing the internal of the aircraft.
- Research to optimize the weight of the aircraft by using materials with less weight but with the same or better characteristics.
- More researches to find better mechanism that may lead to decreasing the weight.





9.0 References

- [1] UDC Sessions
- [2] [Low-Speed-Airfoil-Data-V1.pdf \(illinois.edu\)](https://low-speed-airfoil-data-v1.pdf)
- [3] [Omni Calculator](#)
- [4] <https://apogeerockets.com/education/downloads/Newsletter149.pdf>





10.0 MATLAB Code

```
%>>> %% Constraints
%Max MTOW = 2.5 Kg
%Max span (b) = 1.6 m
%Max airfoil thickness = 0.0045 m

%% Don't Go Far From the Following Ranges
%Cruise speed ranges from 13 to 18 m/s
%Stall speed ranges from 5 to 8 m/s (the lower the better)
%V_HT ranges from 0.3 to 0.6
%V_VT ranges from 0.02 to 0.05
%SH/Sw ranges from 0.2 to 0.25
%AR_VT is 3
%AR_HT is 3

%% Design mission
%Light weight as much as possible (small areas)
%High range and endurance to achieve the 3 laps goals
%High V_cruise

%Remember that for electrically powered UAVs (like ours), Because their
%weight remains the same, In this case the goal is to minimize the total
%power required from the battery
%The endurance then = battery output power (watt) / tot. power req. (watt)
%The range then = endurance * V_cruise

%% ***** Inputs *****
clc
clear all
close all

rho = 1.225; % Denisty
meu = 1.5e-5; % Kinematic Viscosity

MTOW = 2.3 * 9.8; % Max Takeoff weight
V_stall = 7.75; % Stall velocity

%Airfoil
CL_max = 1.52; % Max lift coeff
CL_cruise = 0.4; % Cruise lift coeff
AR = 6.25; % wing aspect ratio

SH_to_Sw = 0.205; % Horizontal tail area
to wing area ratio
V_HT = 0.6; % Horizontal tail
volumetric ratio
```





```
AR_H = 3; % Horizontal tail aspect ratio

V_VT = 0.05; %% Vertical tail volumetric ratio
AR_V = 3; %% Vertical tail aspect ratio

TR = 1; %% Taper ratio
Sweep = 0; %% Sweep
Root_Twist = 0; %% Twist

%% ***** Design Parameters *****
DP_1(1,:)={"WingArea","Stall Speed","Max Lift Coeff","Cruise Lift Coeff"};

Sw = MTOW/(0.5*rho*(V_stall^2)*CL_max);
b = sqrt(Sw * AR);
Cw = b / AR;

Para(1,1) = double(Sw);
DP_1(2,1) = {Sw};

Para(1,2) = double(V_stall);
DP_1(2,2) = {V_stall};

Para(1,3) = double(CL_max);
DP_1(2,3) = {CL_max};

Para(1,4) = double(CL_cruise);
DP_1(2,4) = {CL_cruise};

fprintf("The Design data depending on your chosen design parameters are
shown in an excel sheet \nCalled 'Iteration 1' for better visualization \nIf
you're going to change your design parameters \nSave the important results
somewhere else\n\n")
writecell(DP_1,'Iteration 1.xlsx','Sheet',1,'Range','A1')

%% ***** Wing Size *****
DP_2(1,:)={"Aspect Ratio","Taper Ratio","Wing Area","Span","Root Chord","Tip
Chord","MAC"};

DP_2(2,1) = {AR};
DP_2(2,2) = {TR};
DP_2(2,3) = {Sw};
b(1) = sqrt(AR*Sw);
DP_2(2,4) = {b};

Cr(1) = (2 * Sw)/(b*(1 + TR));
DP_2(2,5) = {Cr};
```





```
Ct(1) = TR * Cr;
DP_2(2,6) = {Ct};

MAC(1) = (2/3) * Cr * ((1 + TR + TR^2)/(1 + TR));
DP_2(2,7) = {MAC};

writecell(DP_2,'Iteration 1.xlsx','Sheet',1,'Range','A4')

%% ***** Tail Size *****
DP_3(1,:)={"Wing Area","MAC","Wing Span","HT Vol. Ratio","HT AR","HT Area / Wing Area","HT Area","HT Arm","HT Span","HT Chord","VT Vol. Ratio","VT AR","VT Arm","VT Area","VT Span","VT Chord"};

DP_3(2,1) = {Sw};
DP_3(2,2) = {MAC};
DP_3(2,3) = {b};

DP_3(2,4) = {V_HT};
DP_3(2,5) = {AR_H};
DP_3(2,6) = {SH_to_Sw};

SH = Sw * SH_to_Sw;
DP_3(2,7) = {SH};

LH = V_HT * Sw * MAC / SH;
DP_3(2,8) = {LH};

bH = sqrt(AR_H * SH);
DP_3(2,9) = {bH};

CH = bH / AR_H;
DP_3(2,10) = {CH};

DP_3(2,11) = {V_VT};
DP_3(2,12) = {AR_V};

LV = LH;
DP_3(2,13) = {LV};

SV = (V_VT * Sw * b) / LV;
DP_3(2,14) = {SV};

bV = sqrt(AR_V * SV);
DP_3(2,15) = {bV};

CV = bV / AR_V;
DP_3(2,16) = {CV};
```





```
writecell(DP_3,'Iteration 1.xlsx','Sheet',1,'Range','A7')

%% ***** From XFLR

%static margin = (Xnp - Xcg) / MAC
static_margin = input("Enter Static Margin Percentage: ");
Xnp = input("Enter Neutral Point Coordinate From XFLR: "); % Neutral Point
Xcg = Xnp - (static_margin/100 * MAC); % Center of
gravity

fprintf("Put The Xcg in the XFLR analysis at %.5f \n\n",Xcg)

%% From V vs Cm graph at Cm = 0 (Trim)
DP_4(1,:) = {"Trim angle", "Take-Off Velocity", "Cruise Velocity", "Max
Velocity", "Cruise Reynolds", "Max Reynolds", "Static Margin", "Xnp", "Xcg"};

trim_angle = input("Enter trim angle from XFLR: ");
DP_4(2,1) = {trim_angle};

V_TO = 1.3 * V_stall; % Take-off velocity
DP_4(2,2) = {V_TO};

V_cruise = input("Enter V_cruise from XFLR: ");
DP_4(2,3) = {V_cruise};

V_max = 1.3 * V_cruise; % Max velocity
DP_4(2,4) = {V_max};

Re_cruise = V_cruise * MAC / meu; % Reynolds number at cruise
DP_4(2,5) = {Re_cruise};

Re_max = V_max * MAC / meu; % Max Reynolds number
DP_4(2,6) = {Re_max};

DP_4(2,7) = {static_margin};
DP_4(2,8) = {Xnp};
DP_4(2,9) = {Xcg};
writecell(DP_4,'Iteration 1.xlsx','Sheet',1,'Range','A10')

%% ***** Moment of inertia estimation
% To be revised

DP_5(1,:) = {"Aircraft Length", "Ixx", "Iyy", "Izz", "Ixz"};
AC_length = CH + LH + Cw; %tail chord + tail arm + wing chord
DP_5(2,1) = {AC_length};

r_Ixx = 0.11 * b;
Ixx = (MTOW/9.8) * r_Ixx^2;
```





```
DP_5(2,2) = {Ixx};

r_Iyy = 0.175 * AC_length;
Iyy = (MTOW/9.8) * r_Iyy ^ 2;
DP_5(2,3) = {Iyy};

r_Izz = 0.19 * (b + AC_length);
Izz = (MTOW/9.8) * r_Izz ^ 2 ;
DP_5(2,4) = {Izz};

Ixz = 0;
DP_5(2,5) = {Ixz};

writecell(DP_5,'Iteration 1.xlsx','Sheet',1,'Range','A13')

%***** Drag estimation *****
% To be revised
Cf = 1.328 / sqrt(Re_cruise);

tc_W = 12/100;
XCm_W = 29.03/100;

tc_t = 7/100;
XCm_t = 29.03/100;

FF_W = 1 + (0.6 / XCm_W) * tc_W + 100 * tc_W^4;
FF_t = 2 * (1 + (0.6 / XCm_t) * tc_t + 100 * tc_t^4);

FF = FF_W + FF_t;

Swet_W = 2 * (1 + 0.2 * tc_W) * Sw;
Swet_t = 2 * (1 + 0.2 * tc_t) * (0.136030131 + 0.095221091);

Swet = Swet_W + Swet_t;

Cdo = Cf * FF * Swet / Sw;

% Thrust required
%CDTO: Drag coefficient during T-0 run --> T-0 == Takeoff
%V_LOF: Liftoff speed == 1.1 V_stall to 1.3 V_stall
%Vo is equal to hand speed at launching

W_per_S = MTOW / Sw;
Cdo = 0.04;
e = 0.8;
K = 1 / (pi * e * AR);
V_LOF = 1.2 * V_stall;
Vo = 5;
```





```
v_q = (V_LOF - Vo)/sqrt(2);
q = 0.5 * rho * v_q^2 ;
Sg = 5;
CDTo = Cdo + K * CL_max^2;
g=9.8;
sigma = 1;
T_static = ( MTOW * (((((V_LOF)^2)-Vo^2)/(2 * g * Sg)) + (q*CDTo)/(W_per_S))
)/9.8;
T_dynamic_max = ( MTOW * ( (rho * V_max ^ 2 * Cdo * (0.5 / W_per_S)) + ((2 *
K * W_per_S) / (rho * sigma * V_max ^ 2)) )/9.8;
T_dynamic_cruise = ( MTOW * ( (rho * V_cruise ^ 2 * Cdo * (0.5 / W_per_S)) +
((2 * K * W_per_S) / (rho * sigma * V_cruise ^ 2)) )/9.8;

% Phase 2

MTOW2 = 1.4 * 9.8;
W_per_S2 = MTOW2 / Sw;

DP_6(1,:) ={"V_Stall2", "Trim angle 2", "Take-Off Velocity 2", "Cruise
Velocity 2", "Max Velocity 2", "Cruise Reynolds", "Max Reynolds 2", "Static
Margin 2", "Xnp 2", "Xcg 2"};

V_stall2 = sqrt( MTOW2 /(0.5 * rho * Sw * CL_max));
DP_6(2,1) = {V_stall2};

trim_angle2 = input("Enter trim angle from XFLR: ");
DP_6(2,2) = {trim_angle2};

V_T02 = 1.3 * V_stall2 ; % Take-off velocity
DP_6(2,3) = {V_T02};

V_cruise2 = input("Enter V_cruise from XFLR: ");
DP_6(2,4) = {V_cruise2};

V_max2 = 1.3 * V_cruise2; % Max velocity
DP_6(2,5) = {V_max2};

Re_cruise2 = V_cruise2 * MAC / meu; % Reynolds number at cruise
DP_6(2,6) = {Re_cruise2};

Re_max2 = V_max2 * MAC / meu; % Max Reynolds number
DP_6(2,7) = {Re_max2};

DP_6(2,8) = {static_margin};
DP_6(2,9) = {Xnp};
DP_6(2,10) = {Xcg};
writecell(DP_6,'Iteration 1.xlsx','Sheet',1,'Range','A16')
```





```
Cf = 0.455 / ( log10(Re_cruise) ^ 2.58);

f = L_fuselage / sqrt( (4 / pi) * Amax_fuselage);

FF_F = 1 + (60 / f^3) + (f/400);
FF_W = 1 + (0.6 * tc_W / XCm_W) + (100 * (tc_W ^ 4) );
FF_VT = 1 + (0.6 * tc_VT / XCm_VT) + (100 * (tc_VT ^ 4) );
FF_HT = 1 + (0.6 * tc_HT / XCm_HT) + (100 * (tc_HT ^ 4) );

FF = FF_F + FF_W + FF_VT + FF_HT;

Swet_F = 4 * Amax_fuselage;
Swet_W = 2 * (1 + (0.2 * tc_W) ) * app.Sw;
Swet_VT = 2 * (1 + (0.2 * tc_VT) ) * app.SV;
Swet_HT = 2 * (1 + (0.2 * tc_HT) ) * app.SH;

Swet = Swet_F + Swet_W + Swet_VT + Swet_HT;

app.Cdo = 1.15 * ( (Cf * FF * Swet) / app.Sw );

K = 1 / (pi * app.e * app.AR);

Cdi = K * (CL ^ 2);

Cd = Cdi + app.Cdo;

W_per_S = app.MTOW / app.Sw;

app.V_cruise = (Re_cruise * app.meu) / app.MAC;
V_max = 1.3 * app.V_cruise;

K = 1 / (pi * app.e * app.AR);
V_LOF = 1.2 * app.V_stall;
Vo = 5;
v_q = (V_LOF - Vo)/sqrt(2);
q = 0.5 * app.rho1 * v_q^2 ;
Sg = 5;
CDTo = app.Cdo + K * app.CL_max^2;
g=9.8;
sigma = 1;
T_static = ( app.MTOW * (((((V_LOF)^2)-Vo^2)/(2 * g * Sg)) +
(q*CDTo)/(W_per_S)) )/9.8;
T_dynamic_max = ( app.MTOW * ( (app.rho1 * V_max ^ 2 * app.Cdo * (0.5 /
W_per_S)) + ((2 * K * W_per_S) / (app.rho1 * sigma * V_max ^ 2)) ))/9.8;
T_dynamic_cruise = ( app.MTOW * ( (app.rho1 * app.V_cruise ^ 2 * app.Cdo *
(0.5 / W_per_S)) + ((2 * K * W_per_S) / (app.rho1 * sigma * app.V_cruise ^
2)) ))/9.8;
```

